Supplementary Materials for

Colorectal cancer residual disease at maximal response to EGFR blockade displays a druggable Paneth cell-like phenotype

Barbara Lupo, Francesco Sassi, Marika Pinnelli, Francesco Galimi, Eugenia R. Zanella, Valentina Vurchio, Giorgia Migliardi, Paolo Armando Gagliardi, Alberto Puliafito, Daria Manganaro, Paolo Luraghi, Michael Kragh, Mikkel W. Pedersen, Ivan D. Horak, Carla Boccaccio, Enzo Medico, Luca Primo, Daniel Nichol, Inmaculada Spiteri, Timon Heide, Alexandra Vatsiou, Trevor A. Graham, Elena Élez, Guillem Argiles, Paolo Nuciforo, Andrea Sottoriva, Rodrigo Dienstmann, Diego Pasini, Elena Grassi, Claudio Isella, Andrea Bertotti*, and Livio Trusolino*

*Corresponding authors. E-mails: livio.trusolino@ircc.it; andrea.bertotti@ircc.it

The file includes:

Figure S7. Transcript and protein changes of Paneth-cell markers and global gene expression variations in representative mCRC PDXs during different time points of cetuximab treatment and after therapy suspension

Figure S8. Expression of YAP and YAP targets in representative mCRC PDXs during different time points of cetuximab treatment and after therapy suspension

Figure S9. Inhibition of YAP activity and expression of YAP-dependent genes by cetuximab in CRC cell lines

Figure S10. Expression of secretory/Paneth cell genes after YAP silencing in CRC cell lines

Figure S11. YAP-dependent regulation of Wnt target genes in CRC cell lines

Figure S11. Expression of secretory/Paneth cell genes after YAP silencing in CRC cell lines.

Figure S12. Modulation of YAP transcriptional activity by cetuximab and other inhibitors of the EGFR pathway in CRC cell lines

Figure S13. Expression/activity of doxycycline-inducible YAP-5SA and modulation of secretory/Paneth cell genes by EGFR pathway inhibition in vitro and in vivo

Figure S14. Expression of secretory/Paneth cell genes after YAP silencing or YAP overexpression in vitro and in vivo

Figure S15. Modulation of EGFR family ligands in mCRC PDXs treated with cetuximab

Figure S16. Effects of individual signal inhibition and dual blockade of EGFR and PI3K or EGFR and MEK in CRC cell cultures

Figure S17. Effects of cetuximab on downstream signals in vitro and in vivo

Figure S18. Effects of PI3K inhibitors on downstream signals and tumor growth in vivo

Figure S19. Effects of PI3K inhibition and combined EGFR and PI3K inhibition on mCRC PDX macroscopic residual disease (pre-treatment and end-of-treatment tumor volumes)

Figure S20. Effects of combined EGFR and PI3K inhibition on mCRC PDX microscopic residual disease, apoptosis, and survival

Figure S21. YAP-dependent transcriptional modulation of *HER2* and *HER3* in CRC cell lines

Figure S22. Modulation of *HER2* and *HER3* expression in mCRC PDXs during prolonged treatment with cetuximab

Figure S23. DEFA5 and HER2/HER3 double staining in representative mCRC PDXs treated with cetuximab

Figure S24. CRC cell line sensitivity to individual targeting of HER family members

Figure S25. Effects of cetuximab and Pan-HER on EGFR downstream targets in vivo

Other Supplementary Material for this manuscript includes the following:

Data file S1 (Microsoft Excel format). List of genes subject to mutational and gene copy number analysis

Data file S2 (Microsoft Excel format). GSEA of gene expression changes induced by cetuximab in mCRC PDXs

Data file S3 (Microsoft Excel format). Ingenuity pathway analysis of gene expression changes induced by cetuximab in mCRC PDXs

Data file S4 (Microsoft Excel format). Expression changes of secretory/Paneth cell genes induced by cetuximab in the reference collection (GSE108277)

Data file S5 (Microsoft Excel format). Original data

Data file S6 (Microsoft Excel format). Taqman probes used for RT-qPCR

SUPPLEMENTARY MATERIALS AND METHODS

ChIP-seq analysis of PDXs

Frozen PDX samples were disaggregated in ice-cold PBS in the presence of protease inhibitors. Tumor suspensions were cross-linked first with 2 mM disuccinimidyl glutarate (Covachem) and then with 1% formaldehyde (Fisher). Chromatin was sonicated in IP Buffer (100 mmol/L Tris pH

8.6, 0.3% SDS, 1.7% Triton X-100, and 5 mmol/L EDTA) to an average length of 500-1000 bp. Samples were immunoprecipitated overnight at 4°C with a rabbit anti-β-catenin antibody (Cell Signaling Technology). Purified DNA was sonicated to an average length of 200 bp and used for library preparation. Sequencing data were analyzed using QARI and PMS modules of the EpiMINE software (56).

Immunohistochemistry and morphometric analyses

Tumors were formalin-fixed, paraffin-embedded, and subjected to hematoxylin-and-eosin or immunoperoxidase staining with the following antibodies: mouse anti-Ki-67 (Dako); rabbit anti-phospho-S6 (Ser235/236), rabbit anti-phospho-ERK (Thr202/Tyr204), rabbit anti-cleaved caspase-3, rabbit anti-pospho-HER2 (Tyr1248), rabbit anti phospho-HER3 (Tyr1289), all from Cell Signaling Technology; mouse anti-α5 defensin (Abcam); mouse anti-YAP (Santa Cruz Biotechnology); mouse anti-β-catenin (BD Biosciences); rabbit anti-β-catenin (Cell Signaling). After incubation with secondary antibodies, immunoreactivities were revealed by incubation in DAB chromogen (Dako). Images were captured with the Leica LAS EZ software using a Leica DM LB microscope. Morphometric quantitation was performed by ImageJ software using spectral image segmentation. For double-staining experiments, the VECTOR® VIP Peroxidase Substrate Kit (Vector Laboratories) was employed. Antigens detected by Phospho-HER2, phospho-HER3, and rabbit β-Catenin antibodies were revealed by rabbit secondary antibody followed by DAB; α5 defensin immunoreactivity was revealed by mouse secondary antibody and VECTOR® VIP purple chromogen. Morphometric quantitation was performed by image J software using color deconvolution segmentation. Software outputs were manually verified by visual inspection of digital images.

Gene expression analyses

For RT-qPCR experiments, total RNA was extracted using the Maxwell® Instrument (Promega) and reverse-transcribed using High-Capacity cDNA reverse transcription (Life Technologies). Results were normalized to the average of two housekeeper genes. The Taqman probes (all provided by ThermoFisher except for ASCL2, which was purchased from Integrated DNA Technologies) are listed in data file S6. For RNA-seq analysis, 1.5 to 2.5 µg RNA were sequenced using the TruSeq stranded mRNA kit from Illumina. FastQ files were processed with the Salmon tool, quality-checked with multiQC and normalized for quality assessment. Principal component analysis was then performed on the gene expression profiles. For microarray experiments, RNA was extracted using the miRNeasy Mini Kit (Qiagen). Synthesis of cDNA and biotinylated cRNA was performed using the IlluminaTotalPrep RNA Amplification Kit (Ambion). Quality assessment and quantitation of total RNA and cRNAs were performed with Agilent RNA kits on a Bioanalyzer 2100 (Agilent). Hybridization of cRNAs was carried out using Illumina Human 48k gene chips (Human HT-12 V4 BeadChip). Array washing was performed by Illumina High Temp Wash Buffer for 10' at 55°C, followed by staining using streptavidin-Cy3 dyes (Amersham Biosciences).

Hybridized arrays were stained and scanned in a Beadstation 500 (Illumina). For bioinformatic analyses of microarray data, probe intensity data were extracted using the Illumina Genome Studio software (Genome Studio V2011.1) and subjected to Loess normalization using the Lumi R package. To minimize the noise, probes that generated detectable signals due to cross-species hybridization of transcripts deriving from murine infiltrates in PDX tissues were removed from the analysis. Finally, for each gene the probe displaying the highest signal variance among those that were detected (Genome Studio detection $P = 0$) was selected for further analyses. GSEA was performed using the dedicated software (software.broadinstitute.org/gsea/index.jsp); the statistical significance of enrichment was estimated based on default settings and 1000 gene permutations. IPA was applied to signatures of genes modulated by cetuximab by at least 2 folds. Enrichment (chi-square *P*) was estimated against the "large intestine" and "colon cancer cell lines" background provided by the IPA software. Gene expression microarray data generated in the course of this study have been deposited in the GEO database with accession number GSE108277.

Genomic analyses

For WES, exome libraries were generated from 200 ng DNA using the Agilent SureSelectXT2 Human All Exon V5 Kit and were sequenced on the Illumina HiSeq2500 platform. Median coverage achieved after duplicates was 45x and 62x for CRC0252 and CRC0542, respectively. Adapter trimming was performed with Skewer v0.1.126 with minimum read length after trimming of 35 and mean quality value before trimming of 10. Trimmed reads were aligned to the full human reference genome hg19 with Burrows-Wheeler Aligner (BWA) v0.7.12. PCR duplicates were marked using Picard tools. Joint mutation calling between multiple samples from the same patient was performed using Platypus v0.8.1. Previously sequenced normal sample was used as reference for somatic variant calling (20). The following filtering criteria were used to call somatic variants in WES samples: i) only variants with Platypus filter PASS, alleleBias, Q20, QD, SC and HapScore were kept; ii) minimum coverage and genotype quality of 10 was required; iii) variants in segmental duplicated regions and centromeric regions were removed; iv) a minimum of 3 reads covering the variant in at least one of the tumor samples per patient were considered; v) 0 number of reads covering the variant in the germline sample; and vi) genotype 0/0 in the germline sample. Only somatic alterations and indels with a variant allele frequency higher than 5% were considered.

Cell cultures, reagents, vectors, viral infection, and YAP reporter assays

NCI-HCA46 cells were purchased from Sigma Aldrich and were cultured in DMEM; DiFi cells (from J. Baselga) were cultured in F12. The genetic identity of cell lines was validated by short tandem repeat profiling (Cell ID, Promega). CRC0078 colospheres were maintained as described (57) in the presence of 20 ng/ml EGF. BTC and doxycycline were from Sigma Aldrich. Targeted agents for in vivo or in vitro studies included: cetuximab (Merck); trastuzumab (Roche); Pan-HER and the isolated HER2 and HER3 components of Pan-HER (Symphogen); selumetinib, dactolisib, alpelisib (Carbosynth); BMS345541, ruxolitinib, PLX4720, everolimus, pictilisib, MK2206, and buparlisib

(Selleck Chemicals). YAP-5SA (mutation sites: S61A, S109A, S127A, S164A, S381A) was cloned into the PS100069 lentiviral vector (Origene) for constitutive expression and into the Lenti-X™ Tet-One™ Inducible Expression System-Puro (Takara) for doxycycline-regulated expression. The lentiviral vector expressing Myc-DDK-tagged wild type YAP was provided by Origene. The MISSION YAP-targeting shRNAs, as well as the non-targeting control vector, were from Sigma Aldrich. The sequence of YAP-targeting shRNAs is the following:

YAP_shRNA-1:

CCGGGCCACCAAGCTAGATAAAGAACTCGAGTTCTTTATCTAGCTTGGTGGCTTTTTG

YAP_shRNA-2:

CCGGCAGGTGATACTATCAACCAAACTCGAGTTTGGTTGATAGTATCACCTGTTTTTG.

The TOP-GFP lentiviral vector was a gift from Laurie Ailles (Princess Margaret Cancer Center, University Health Network, Toronto, Canada). Lentiviral vectors were produced by LipofectAMINE 2000 (Invitrogen)-mediated transfection of 293T cells (ATCC): To evaluate YAP activity, cells at 80 % confluence were transiently transfected with the 8xGTIIC-luc YAP-reporter construct (Addgene) using LipofectAMINE 2000. Luciferase activity was assayed 72 h after transfection using the Luciferase Assay System (Promega) and a GloMax 96 microplate luminometer (Promega). For determination of 8xGTIIC-luciferase plasmid concentration, equivalent volumes of DNA were used. DCts were obtained by a 40-Ct transformation, and relative expression levels were expressed as 2^DDCt (median centered).

Biological assays

On day 0, cells were plated at clonal density (20 cells/µl) in complete medium (for CRC0078, EGF was reduced to 4 ng/ml). On day 1, cells were treated as indicated in the figure legends. On day 2, apoptotic activity was measured using the caspase-Glo 3/7 luminescent assay kit (Promega). Results were normalized against viable cells, which were plated in parallel, treated with the same modalities, and assessed by ATP content (Cell Titer-Glo, Promega). Viability assays in the presence of BTC, cetuximab, trastuzumab, Pan-HER, or the isolated HER2 and HER3 components of Pan-HER were conducted for 72 h. Cell numbers were quantitated by ATP content. EDU incorporation in vitro was assessed using the Click-iT™ Plus EdU Cell Proliferation Kit for Imaging, Alexa Fluor™ 488 dye (Life Technologies). Organoids were incubated for 3 hours with 10 µM EdU prior to fixation and permeabilization; then, cells were stained with DAPI. EDU incorporation in vivo was examined by intraperitoneal injection (75 µg). Mice were sacrificed after 24h, and then tumors were explanted, formalin-fixed, paraffin-embedded and processed as described in (58).

Western blot analysis

Proteins were extracted with cold EB buffer (50 mmol/L Hepes pH 7.4, 150 mmol/L NaCl, 1% Triton X-100, 10% glycerol, 5 mmol/L EDTA, 5 mmol/L EGTA) in the presence of phosphatase and protease inhibitors. Lysates were run on precasted SDS-polyacrylamide gels (Invitrogen) and transferred to nitrocellulose membranes using a Trans-Blot Turbo Blotting System (Biorad). Membrane-bound antibodies were detected by the enhanced chemiluminescence system (Promega). Primary antibodies were the following: rabbit anti-phosho-EGFR (Tyr1068) (Abcam); rabbit anti-EGFR, rabbit anti-phospho-HER2 (Tyr1248), rabbit anti-phospho-HER3 (Tyr1289), rabbit anti-phospho-AKT (Ser473), rabbit anti-AKT, rabbit anti-phospho-ERK (Thr202/Tyr204), rabbit anti-ERK, rabbit anti-phospho-YAP (Ser127), rabbit anti-phospho-YAP (Ser397), all from Cell Signaling Technology; mouse anti-vinculin and mouse anti-α-tubulin (Sigma-Aldrich); mouse anti-c-Myc Tag, rabbit anti-YAP, and mouse anti-HER2, both from Santa Cruz Biotechnology; mouse anti-HER3 (Millipore).

SUPPLEMENTARY FIGURES

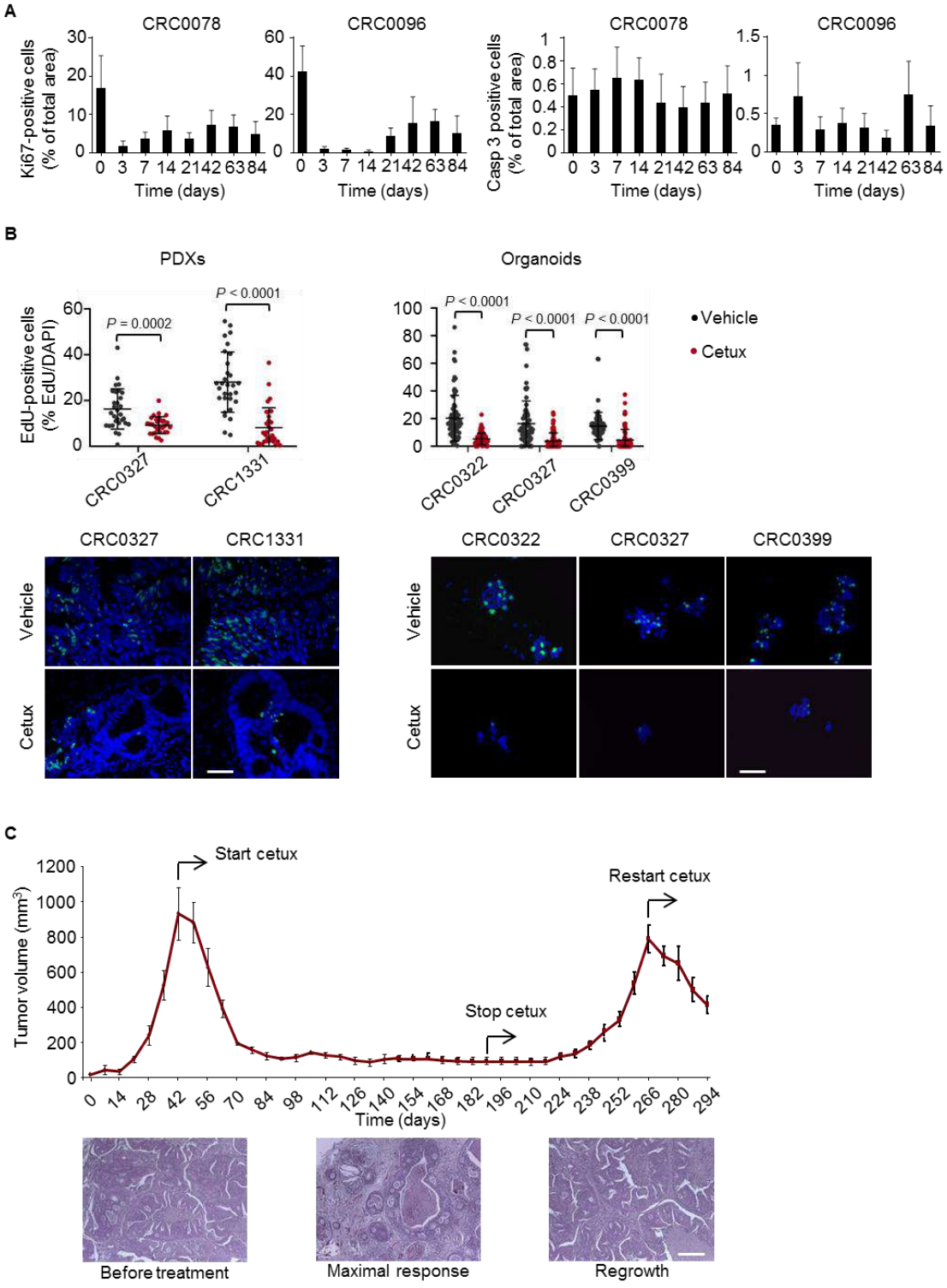

Figure S1. Biological characterization of residual disease after prolonged treatment with cetuximab in representative mCRC PDXs

(**A**) Morphometric quantitation of proliferation (left panels) and apoptosis (right panels) in PDX models CRC0078 and CRC0096 treated with cetuximab (20 mg/kg twice a week intraperitoneally) for 12 weeks. At the indicated times, tumors were explanted and subjected to immunohistochemical analysis. Bars are the means ± SD of 10 optical fields (Ki67, 40X) or 5 optical fields (caspase 3, 20X) for each time point for each tumor (*n* = 20 to 30 for Ki67 and *n* = 5 to 15 for active caspase 3). Casp, caspase. (**B**) Left panels, morphometric quantitation and representative images of EdU incorporation in two PDXs from the reference collection after treatment with vehicle (until tumors reached an average volume of 1500 mm^3) or cetuximab (for 6 weeks). At the end of treatment, 3 tumors from 3 different mice were explanted and subjected to immunohistochemical analysis. Each dot represents the value measured in one optical field, with 10 optical fields per tumor (*n* = 30 for each condition). Right panels, morphometric quantitation and representative images of EdU incorporation in 3 PDX-derived organoids after treatment with vehicle or cetuximab (20 μg/ml) for 2 weeks. Results are the means ± SD of 3 biological replicates. Each dot represents the value measured in one optical field, with 25 optical fields per replicate (*n* = 75). Statistical analysis by two-tailed unpaired Welch's *t*-test. Scale bar, 100 μm (left panels) or 50 μm (right panels). Cetux, cetuximab. (**C**) Upper panel, tumor growth curve showing the response of PDX model CRC0059 over the course of a 21-week treatment with cetuximab, followed by therapy discontinuation and subsequent drug re-challenging. Values indicate the mean tumor volumes ± SEM (*n* = 6). Lower panel, representative hematoxylin-and-eosin images of the same case immediately before treatment, at maximal response (6 weeks), and 11 weeks after drug washout. Before treatment the tumor had a well-differentiated phenotype, with cells describing irregular pluristratified tubular/acinar structures with multiple lumens embedded in a scarce stromal matrix. The post-treatment tissue at maximal response displayed reduced cellularity and pseudoglandular remnants scattered among large necrotic areas. After regrowth, the tumor re-acquired the histopathological characteristics of the treatment-naïve counterpart. Scale bar, 500 μm.

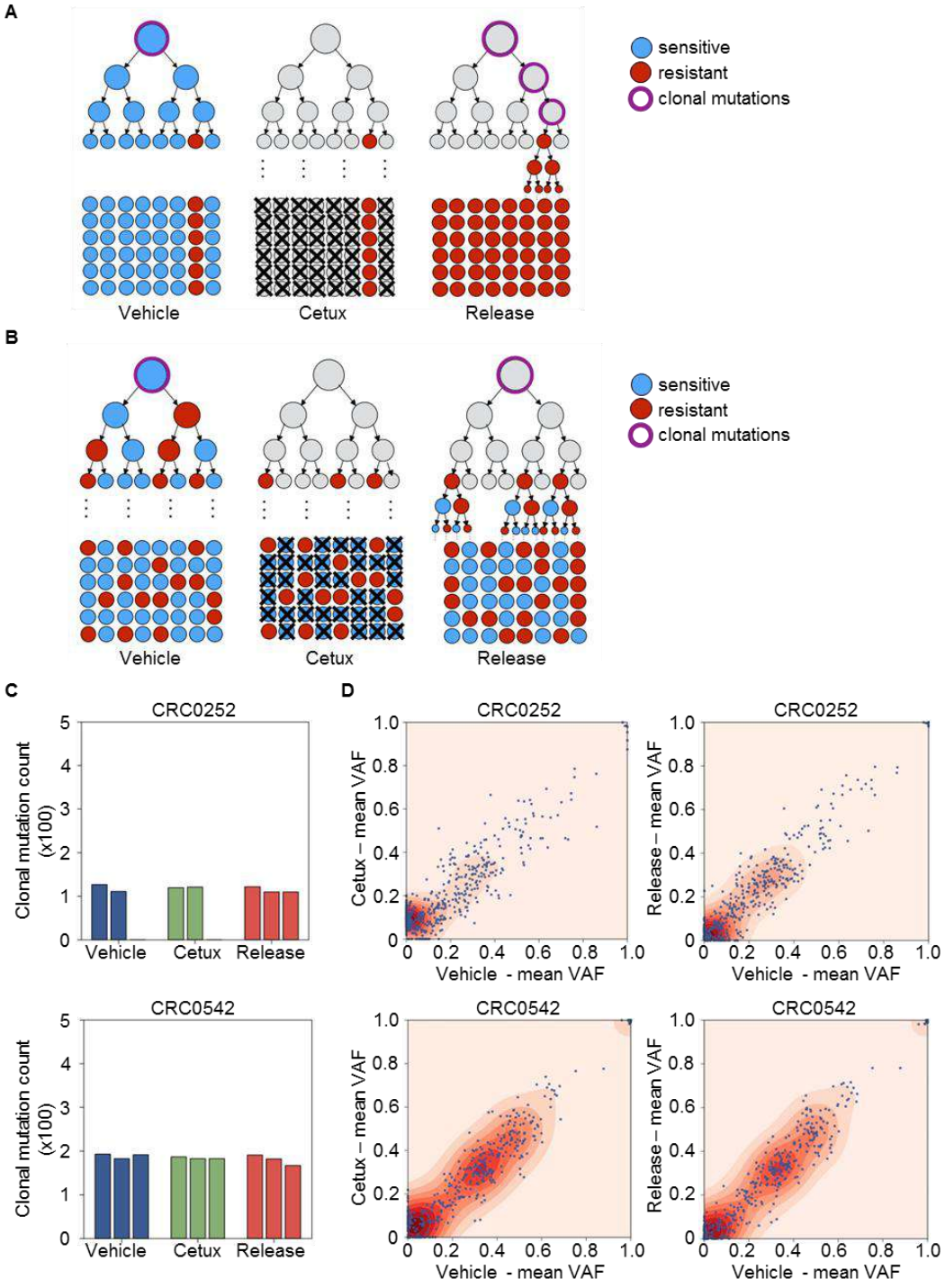

Figure S2. Analysis of adaptive changes *versus* clonal selection induced by cetuximab in representative mCRC PDXs

(**A**) Schematic of the changes in clonal mutational load when drug resistance is heritable (*e.g.* genetically driven). Phylogenetic trees illustrate how selection for a subclonal mutation (subtree, upper right panel) in a heterogeneous population consisting of sensitive (blue dots) and resistant (red dots) cells results in a greater load of clonal/truncal mutations (purple circles) following drug-

induced selection and after therapy cessation, due to the drug-induced population bottleneck. (**B**) Schematic of the changes in clonal mutational load when drug resistance is driven by non-heritable or plastic phenotypes. Nodes in the phylogenetic trees are coloured according to a stochastically determined non-heritable phenotype. Surviving cells are an unbiased sub-sample of the population, leaving the number of clonal/truncal mutations unchanged. Drug exposure initially renders the population homogeneous; however, phenotypic heterogeneity returns when therapy ceases. (**C**) Number of clonal mutations (variant allele frequency greater than or equal to 0.3) detected by whole exome sequencing analysis of untreated tumors (Vehicle), cetuximab-treated samples (Cetux), and tumors that had relapsed following drug withdrawal (Release) in PDX models CRC0252 and CRC0542. Bars refer to the number of replicates. (**D**) Scatter plots showing the mean variant allele frequency of all detected somatic mutations in cetuximab-treated samples and relapsed tumors compared to that detected in untreated tumors. VAF, variant allelic frequency.

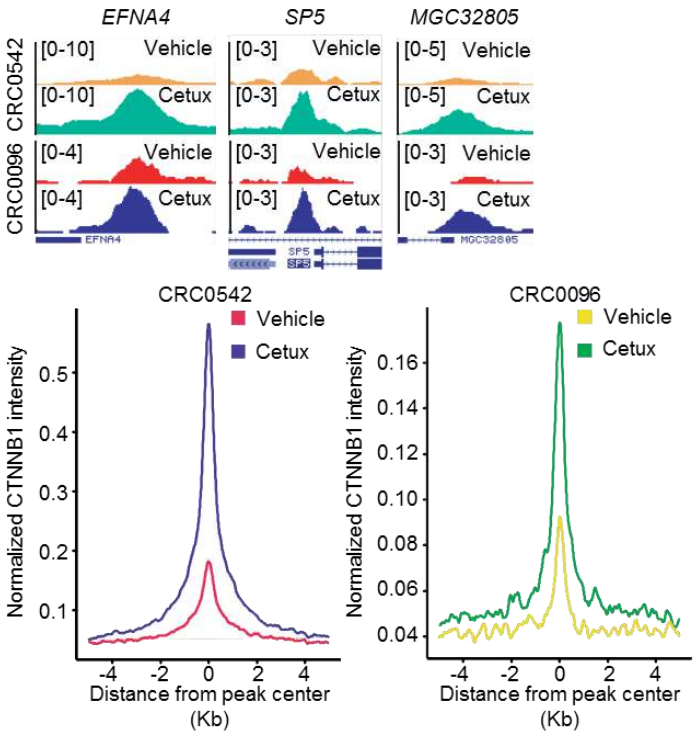

Figure S3. ChIP-seq analysis of residual disease after prolonged treatment with cetuximab in representative mCRC PDXs

Upper panels, genomic snapshots of CTNNB1 ChIP-seq signal at 3 β-catenin target loci from the indicated tumors after treatment with vehicle (until tumors reached an average volume of 1500 mm^3) or cetuximab (for 6 weeks). Lower panels, cumulative CTNNB1 normalized ChIP-seq intensity from the indicated tumors and conditions at CTNNB1-enriched genomic loci +/-4kb to the peak center.

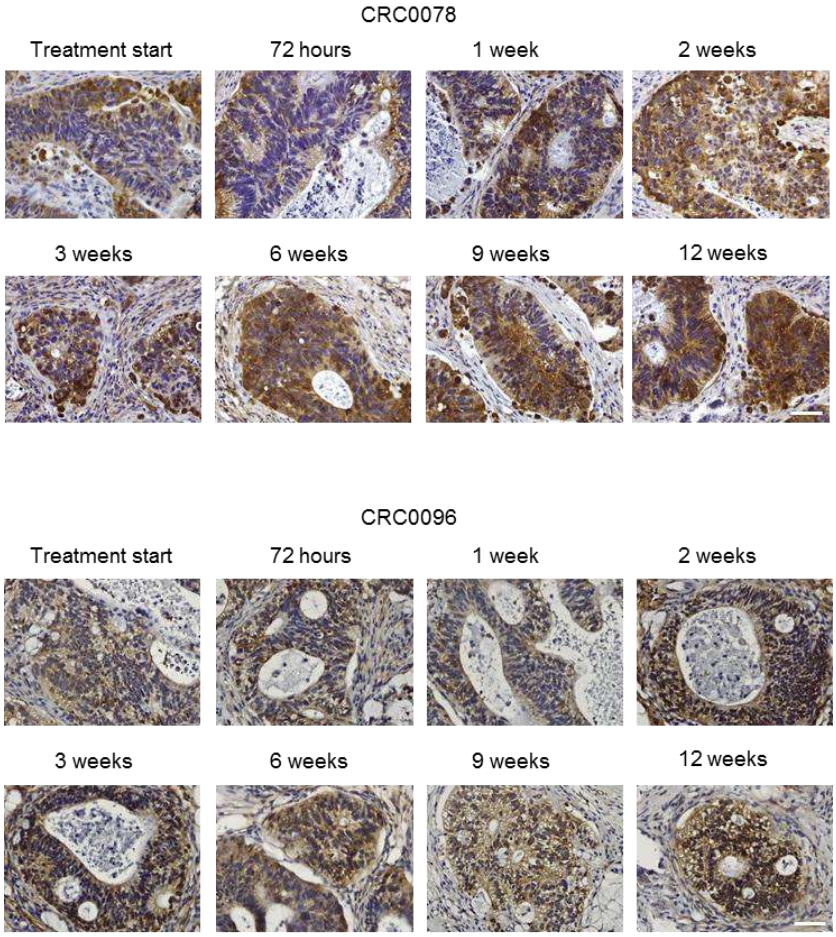

Figure S4. Longitudinal analysis of β-catenin expression at different time points during prolonged treatment with cetuximab in representative mCRC PDXs

Representative images of β-catenin expression and localization in two PDX models treated with cetuximab (20 mg/kg twice a week intraperitoneally) and monitored longitudinally for 12 weeks. At the indicated times, tumors were explanted and subjected to immunohistochemical analysis. Scale bar, 50 μm.

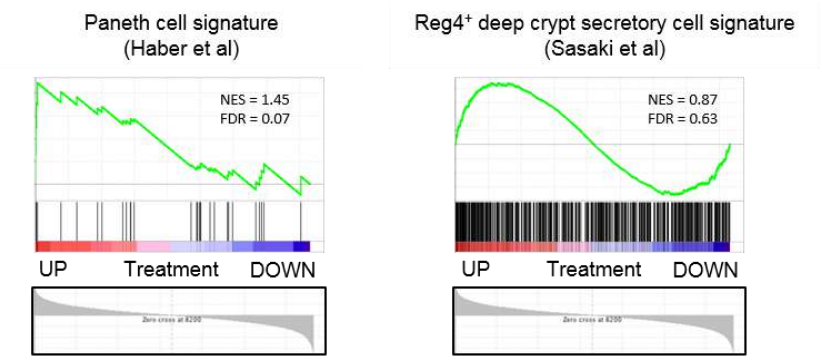

Figure S5. GSEA of residual PDXs with signatures of Paneth cells and deep secretory cells
Left panel: GSEA plot showing positive modulation of a Paneth cell signature, obtained in in the mouse small intestinal epithelium (30), in PDXs treated with cetuximab (GSE108277). Right panel: GSEA plot showing no enrichment for a signature of Reg4^{+} deep crypt secretory cells, which serve as Paneth cell equivalents in the murine colon (31), in PDXs treated with cetuximab. NES, normalized enrichment score; FDR, false discovery rate.

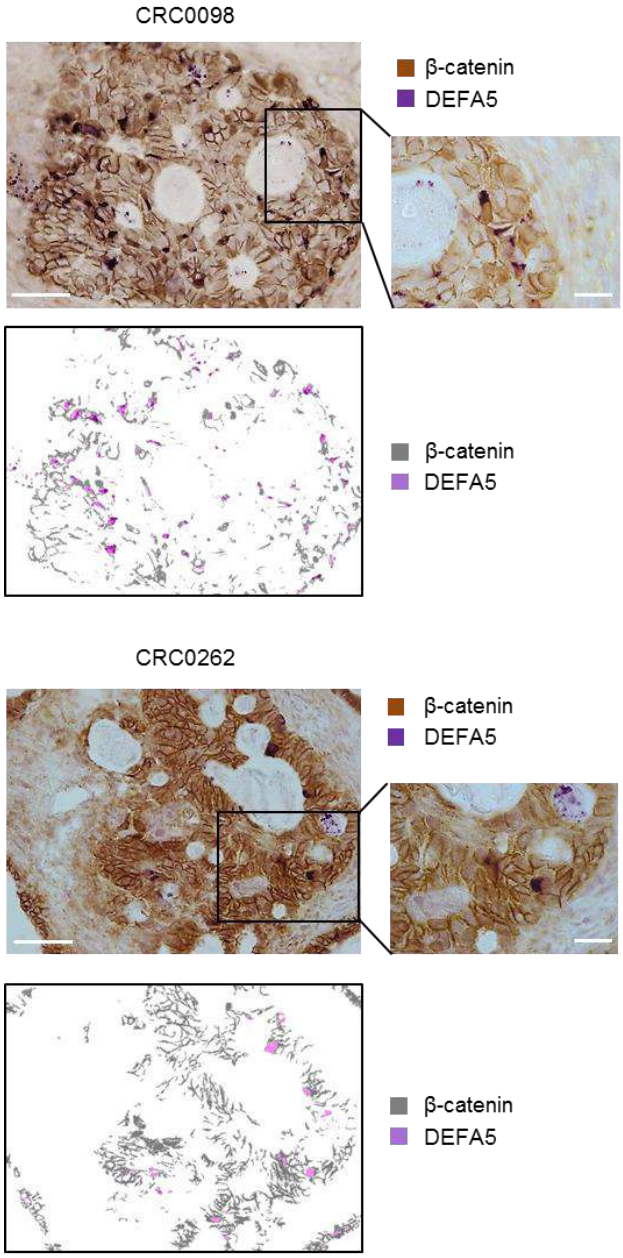

Figure S6. DEFA5 and β-catenin double staining in representative mCRC PDXs treated with cetuximab

DEFA5 and β-catenin double staining in 2 PDX models treated with cetuximab (20 mg/kg twice a week intraperitoneally) for 6 weeks. For each model, the upper panels are representative images of bright-field optical sections. The lower panels show the corresponding color deconvolution segmentation. Scale bar, 50 μM (insets, 20 μM).

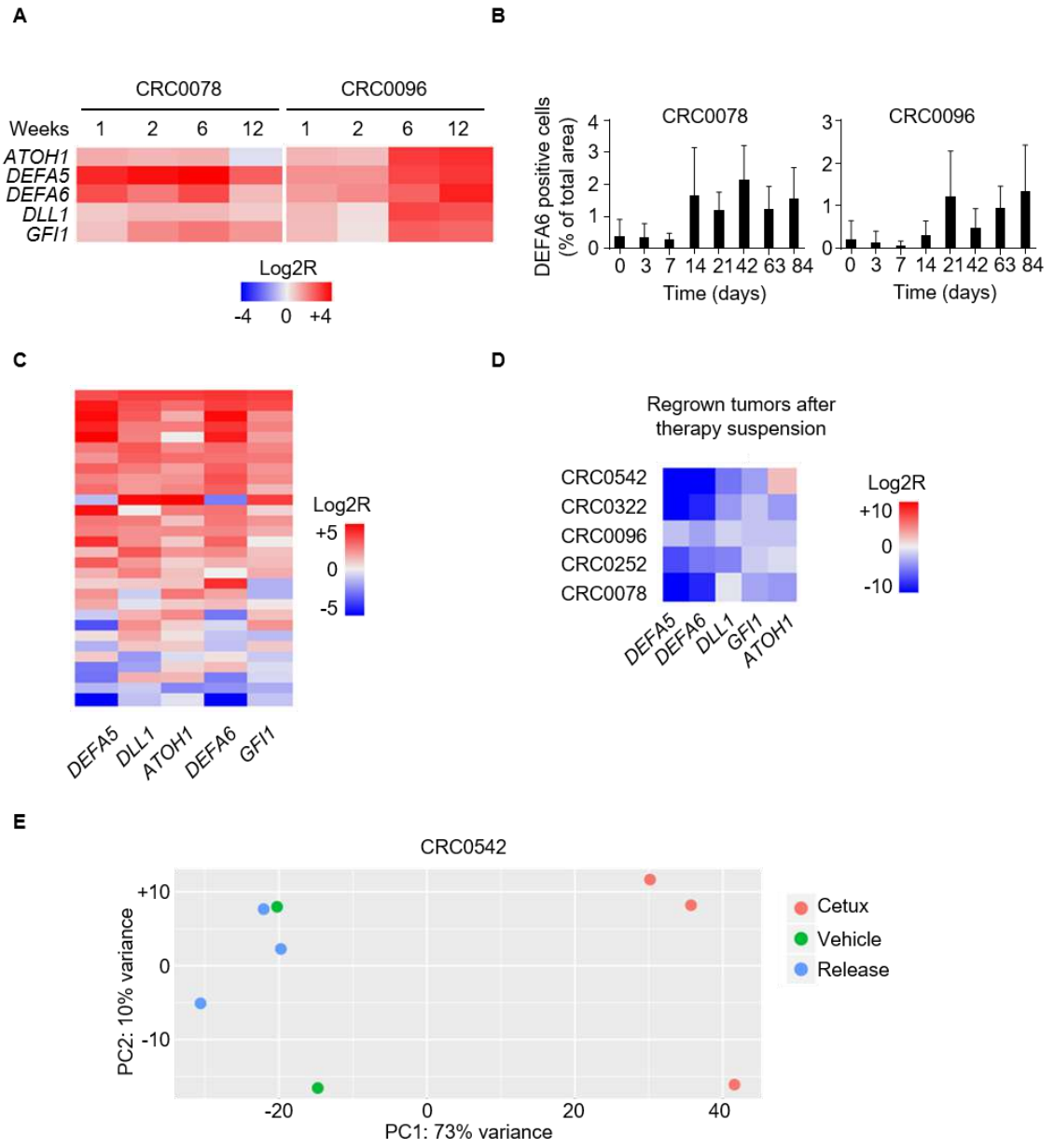

Figure S7. Transcript and protein changes of Paneth-cell markers and global gene expression variations in representative mCRC PDXs during different time points of cetuximab treatment and after therapy suspension

(**A**) Heatmap showing expression changes for the indicated secretory/Paneth cell markers in 2 representative PDXs treated with cetuximab (20 mg/kg twice a week intraperitoneally) and monitored longitudinally for 12 weeks. At the indicated times, 1 tumor from 1 mouse was explanted and subjected to RT-qPCR analysis. Average expression of the 5-gene secretory/Paneth cell signature, Log2R relative to vehicle-treated tumors, for model CRC0078: 1 week, 1.72; 2 weeks, 1.86; 6 weeks, 2.4; 12 weeks, 1.02. Average expression of the 5-gene secretory/Paneth cell signature, Log2R relative to vehicle-treated tumors, for model CRC0096: 1 week, 1.16; 2 weeks,

0.92; 6 weeks, 2.68; 12 weeks, 2.94. (**B**) Morphometric quantitation of DEFA6 protein expression in the 2 PDX models treated with cetuximab and monitored longitudinally for 12 weeks. At the indicated times, tumors were explanted and subjected to immunohistochemical analysis. Bars are the means ± SD of 5 optical fields (20x) for each tumor (n = 5 to 15). (**C**) Heatmap showing expression changes for the indicated secretory/Paneth-cell markers in PDXs of the reference collection after acute treatment with cetuximab (tumor explant 72h after antibody administration), as assessed by RT-qPCR. Average gene expression, Log2R relative to vehicle-treated tumors: *DEFA5* 1.36, $P < 0.0001$; *DLL1* 1.57, $P < 0.0001$; *ATOH1* 1.45, $P < 0.0001$; *DEFA6* 1.31, $P < 0.0001$; *GFI1* 1.01, $P = 0.0001$ by two-tailed Wilcoxon test. Benjamini-Hochberg FDR < 0.1 for all genes. (**D**) Heatmap showing expression changes for the indicated secretory/Paneth-cell markers in 5 representative PDX models after cetuximab withdrawal, when regrown tumors reached volumes of around 750 mm^3. The antibody was discontinued after six weeks of treatment. Gene expression was assessed by RT-qPCR and normalized to cetuximab-treated tumors. Average gene expression of tumors after treatment discontinuation, Log2R relative to cetuximab-treated tumors: *DEFA5* -8.75, $P < 0.0111$; *DEFA6* -7.24, $P = 0.007$; *DLL1* -3.01, $P = 0.0283$; *GFI1* -2.31, $P = 0.0037$; *ATOH1* -1.54, $P = 0.2143$ by two-tailed paired Student's t-test. Benjamini-Hochberg FDR < 0.1 for all genes except *ATOH1*. (**E**) Scatter plot showing the two principal components of transcriptional variance (based on RNAseq analysis) in cetuximab-treated samples (Cetux, red dots), relapsed tumors after therapy discontinuation (Release, blue dots) and untreated tumors (Vehicle, green dots) from PDX model CRC0542. Dots refer to the number of replicates.

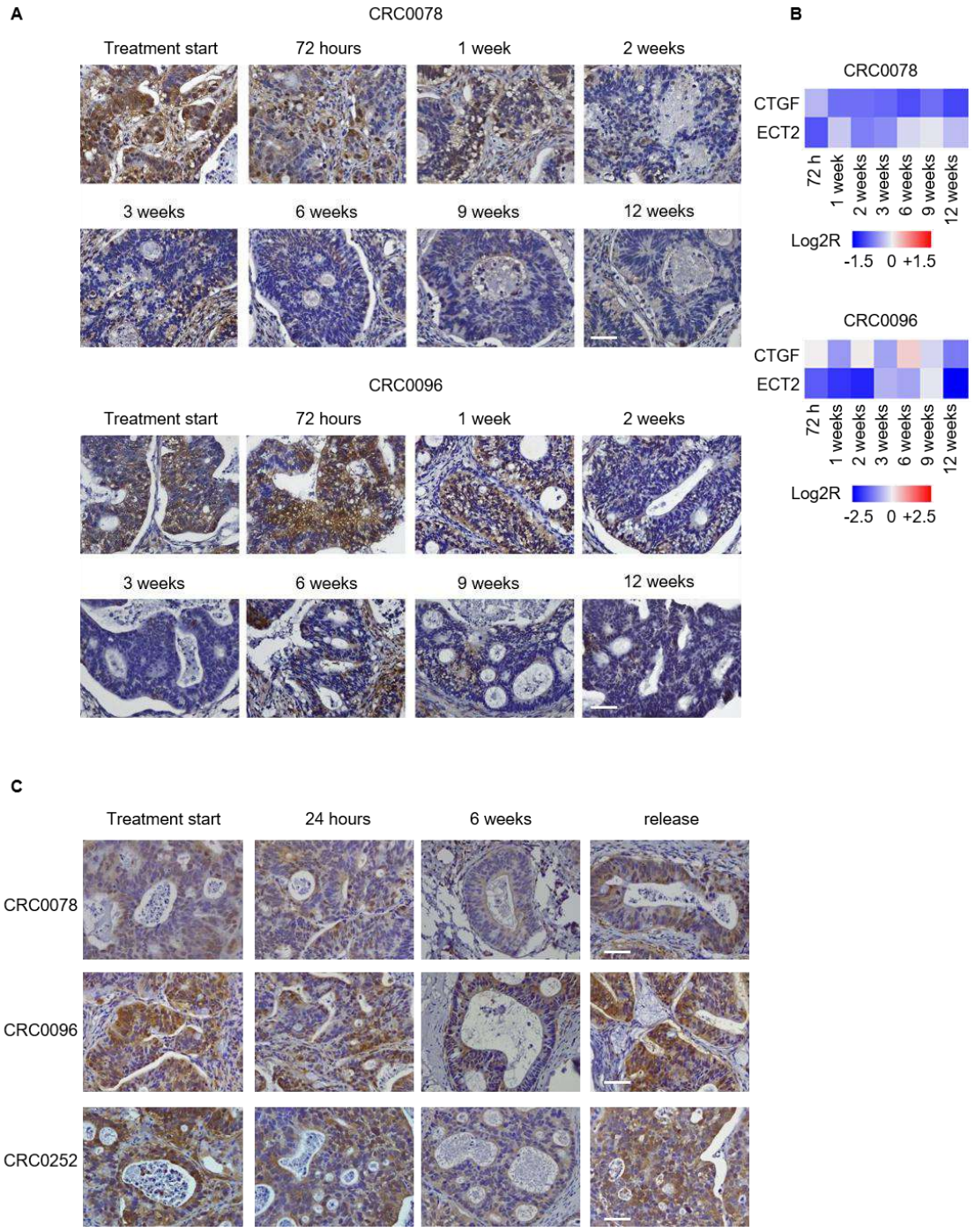

Figure S8. Expression of YAP and YAP targets in representative mCRC PDXs during different time points of cetuximab treatment and after therapy suspension

(**A**) Representative images of YAP expression and localization in 2 PDX models treated with cetuximab (20 mg/kg twice a week intraperitoneally) and monitored longitudinally for 12 weeks. At the indicated times, tumors were explanted and subjected to immunohistochemical analysis. Scale bar, 50 μm. (**B**) Heatmap showing expression changes (assessed by RT-qPCR analysis) for the indicated YAP targets after treatment with cetuximab (20 mg/kg twice a week intraperitoneally) in

the 2 models shown in panel A. At the indicated times, 1 tumor from 1 mouse was explanted and subjected to RT-qPCR analysis. (**C**) Representative images of YAP expression and localization in 3 PDX models after treatment with cetuximab for 24 hours and 6 weeks and after antibody withdrawal, when regrown tumors reached volumes of around 750 mm^3. Scale bar, 50 μm.

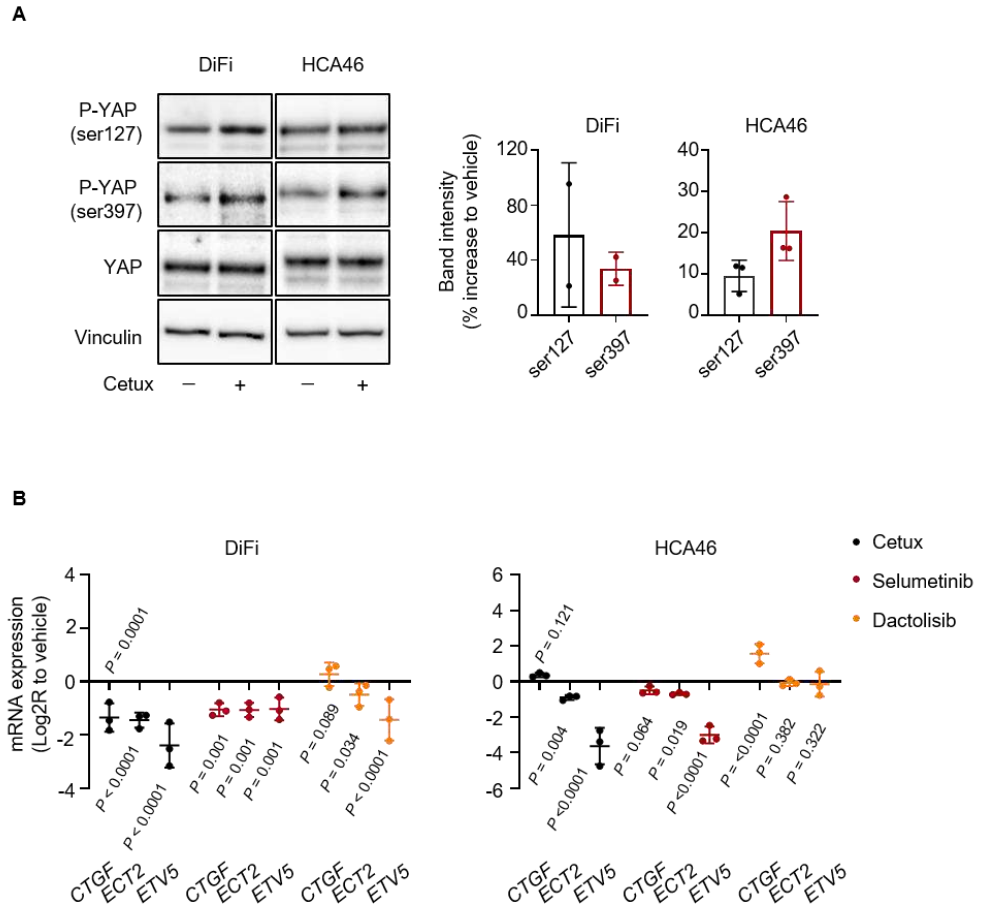

Figure S9. Inhibition of YAP activity and expression of YAP-dependent genes by cetuximab in CRC cell lines

(**A**) Western blot analysis (left) and densitometric quantitation (right) of YAP phosphorylation in DiFi and HCA46 cell lines treated for 1 hour with 20 μg/ml cetuximab. Total YAP was used for normalization; vinculin was used as a loading control. Western blots for total YAP protein were run with the same lysates as those used for anti-phosphoprotein detection but on different gels. The images shown are representative of 2 (DiFi) or 3 (HCA46) experiments on independent biological replicates. The plots of densitometric analysis show means ± range (DiFi) or SD (HCA46), with values normalized against vinculin. P-YAP, phospho-YAP; ser127, serine 127; ser397, serine 397; Cetux, cetuximab. (**B**) RT-qPCR analysis of the indicated YAP target genes in DiFi and HCA46 cells treated for 72h with cetuximab (20 μg/ml), selumetinib (1 μM), or dactolisib (250 nM). Three independent experiments were performed in technical triplicates. The plots show means ± SD. Statistical analysis by one-way ANOVA followed by Benjamini, Krieger and Yekutieli FDR correction.

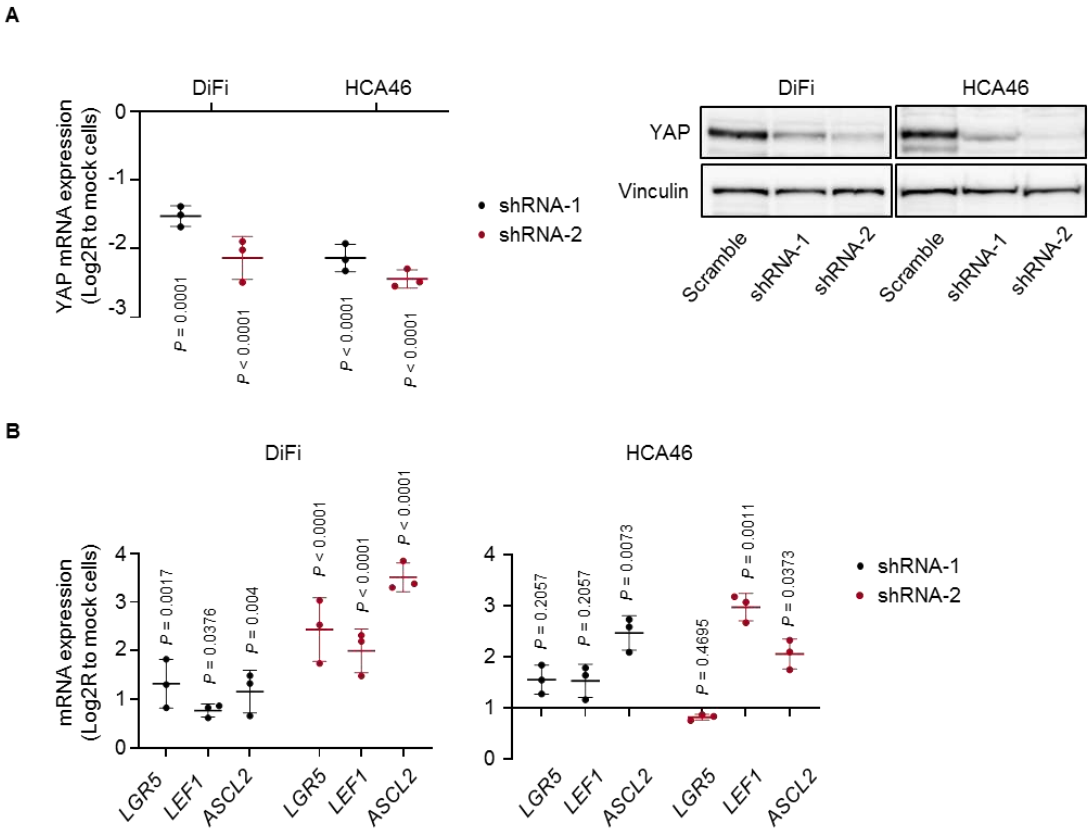

Figure S10. Expression of secretory/Paneth cell genes after YAP silencing in CRC cell lines (**A**) Transcript (left panel) and protein (right panels) expression of YAP in DiFi and HCA46 cells transduced with two different shRNA lentiviral vectors targeting YAP. For RT-qPCR, 3 independent experiments were performed in biological triplicates ($n = 3$). In western blots, vinculin was used as a loading control. Western blot images are representative of 2 experiments on independent biological replicates. (**B**) RT-qPCR analysis of Wnt target gene transcripts in DiFi and HCA46 cells after shRNA-based YAP silencing, compared with mock cells. Three independent experiments were performed in technical triplicates. The plots show means ± SD. Statistical analysis by one-way ANOVA followed by Benjamini, Krieger and Yekutieli FDR correction.

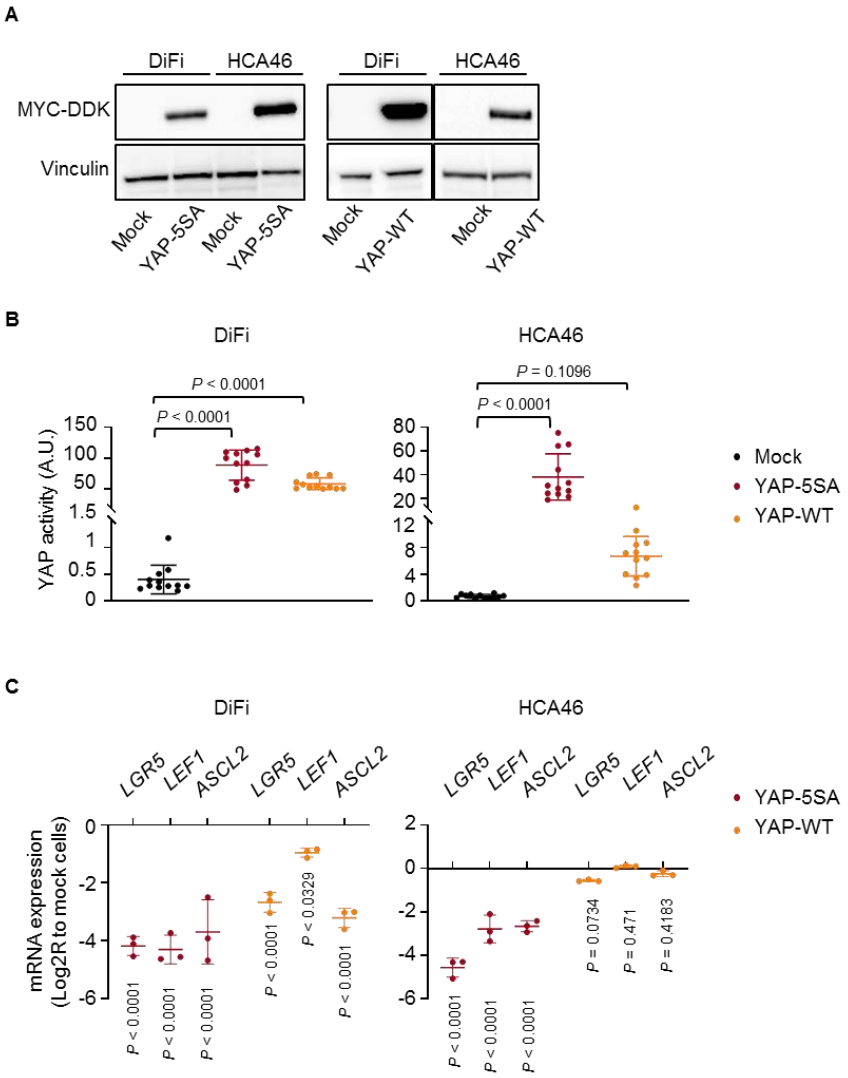

Figure S11. YAP-dependent regulation of Wnt target genes in CRC cell lines

(**A**) Western blot analysis of total protein extracts from DiFi and HCA46 cells transduced with the control pLVX-IRES-Puro vector (mock), a lentiviral vector enabling constitutive expression of the Myc-DDK-tagged mutant YAP variant YAP-S5A (left panels), or a lentiviral vector encoding Myc-DDK-tagged wild-type YAP (YAP-WT) (right panels). YAP-S5A and YAP-WT were detected using a Myc antibody. Vinculin was probed as a loading control. (**B**) Luciferase-based measurement of YAP reporter activity in DiFi and HCA46 cells stably transduced with constitutive YAP-5SA or wild-type YAP and transiently transfected for 72h with the 8xGTIIC-luc YAP-reporter construct. Luciferase activity was normalized against reporter plasmid concentration as determined by DNA qPCR and expressed as arbitrary units (A.U.). Three independent experiments were performed in biological quadruplicates (n = 12). The plots show means ± SD. Statistical analysis by one-way ANOVA followed by Benjamini, Krieger and Yekutieli FDR correction. (**C**) RT-qPCR analysis of the indicated Wnt target genes in DiFi and HCA46 cell lines transduced with YAP-5SA or YAP-WT.

Three independent experiments were performed in technical triplicates. The plots show means ± SD. Statistical analysis by one-way ANOVA followed by Benjamini, Krieger and Yekutieli FDR correction.

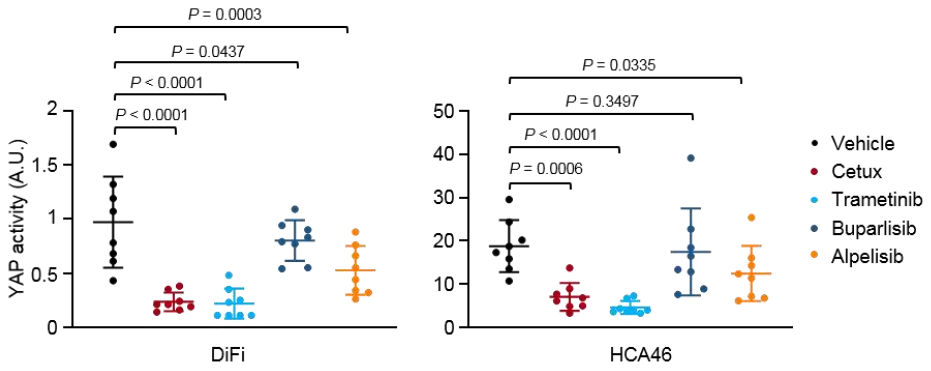

Figure S12. Modulation of YAP transcriptional activity by cetuximab and other inhibitors of the EGFR pathway in CRC cell lines

Measurement of YAP transcriptional activity in DiFi and HCA46 cell lines after treatment for 48h with vehicle (DMSO), cetuximab (20 µg/ml), trametinib (100 nM), buparlisib (0.5 μM), or alpelisib (1 μM). Luciferase activity was normalized against reporter plasmid concentration as determined by DNA qPCR and expressed as arbitrary units (A.U.). Two independent experiments were performed in biological quadruplicates (n = 8). The plots show means ± SD. Statistical analysis by one-way ANOVA followed by Benjamini, Krieger and Yekutieli FDR correction. Cetux, cetuximab.

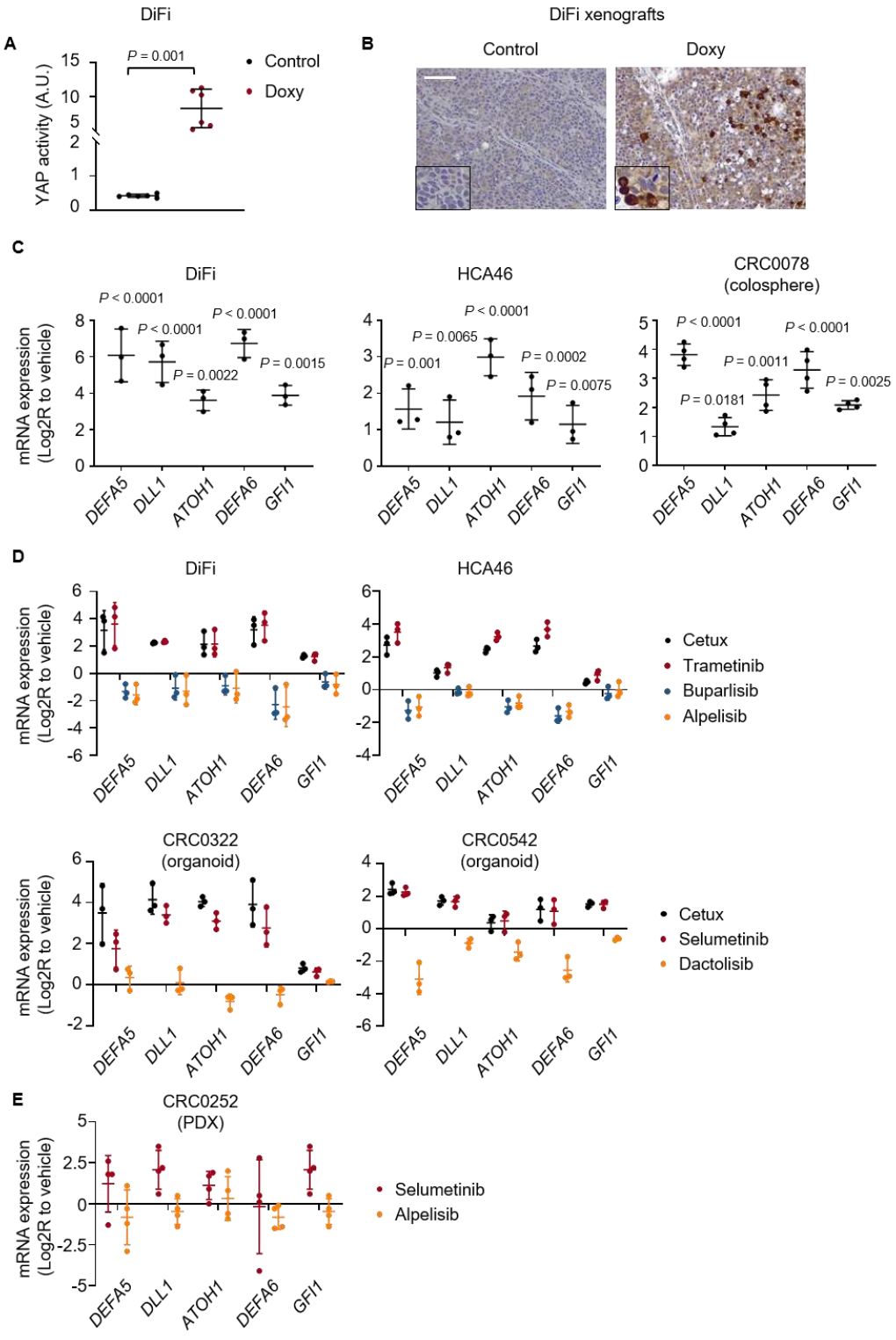

Figure S13. Expression/activity of doxycycline-inducible YAP-5SA and modulation of secretory/Paneth cell genes by EGFR pathway inhibition in vitro and in vivo

(**A**) Luciferase-based measurement of YAP reporter activity in DiFi cells stably transduced with a doxycycline-inducible YAP-5SA Lenti-X™ Tet-One™ Expression System-Puro, transiently

transfected for 72h with the 8xGTIIC-luc YAP-reporter construct, and either left untreated (control) or treated with doxycycline for 48 h. Luciferase activity was normalized against reporter plasmid concentration as determined by DNA qPCR and expressed as arbitrary units (A.U.). Two independent experiments were performed in biological triplicates (n = 6). The plots show means ± SD. Statistical analysis by two-tailed unpaired Welch's t-test. Doxy, doxycycline. (**B**) Representative images of YAP expression in DiFi xenografts after treatment with doxycycline (50 mg/kg daily oral gavage) for 1 week, compared with vehicle-treated (control) counterparts. Scale bar, 100 μm (200 μm for insets). (**C**) RT-qPCR analysis of the indicated Paneth-cell transcripts in CRC cell lines (DiFi and HCA46) and colospheres (CRC0078) treated with 20 μg/ml cetuximab for 72h. Three (DiFi, HCA46) or 4 (CRC0078) independent experiments were performed in technical triplicates. The plots show means ± SD. Statistical analysis by matched one-way ANOVA followed by Benjamini, Krieger and Yekutieli FDR correction. (**D**) RT-qPCR analysis of Paneth-cell transcripts in cell lines and organoids treated with the indicated inhibitors for 72h (cetuximab, 20 μg/ml; selumetinib, 1 μM; trametinib, 100 nM; dactolisib, 250 nM; buparlisib, 0.5 μM; alpelisib, 1 μM). Three independent experiments were performed in technical triplicates. The effects of EGFR and MEK blockade were positively correlated (DiFi, cetuximab *versus* trametinib, $r = 0.997$; HCA46, cetuximab *versus* trametinib, $r = 0.995$; CRC0322, cetuximab *versus* selumetinib, $r = 0.997$; CRC0542, cetuximab *versus* selumetinib, $r = 0.997$, Pearson's correlation coefficient). In contrast, transcriptional changes induced by PI3K pathway inhibition negatively correlated with those triggered by cetuximab (DiFi, cetuximab *versus* buparlisib, $r = -0.832$; cetuximab *versus* alpelisib, $r = -0.855$; HCA46, cetuximab *versus* buparlisib, $r = -0.935$; cetuximab *versus* alpelisib, $r = -0.96$; CRC0322, cetuximab *versus* dactolisib, $r = -0.415$; CRC0542, cetuximab *versus* dactolisib, $r = -0.356$). Cetux, cetuximab. (**E**) RT-qPCR analysis of Paneth-cell transcripts in a PDX model treated for 3 weeks with the indicated inhibitors. Four samples for each condition were analyzed in technical triplicates. The plots show means ± SD.

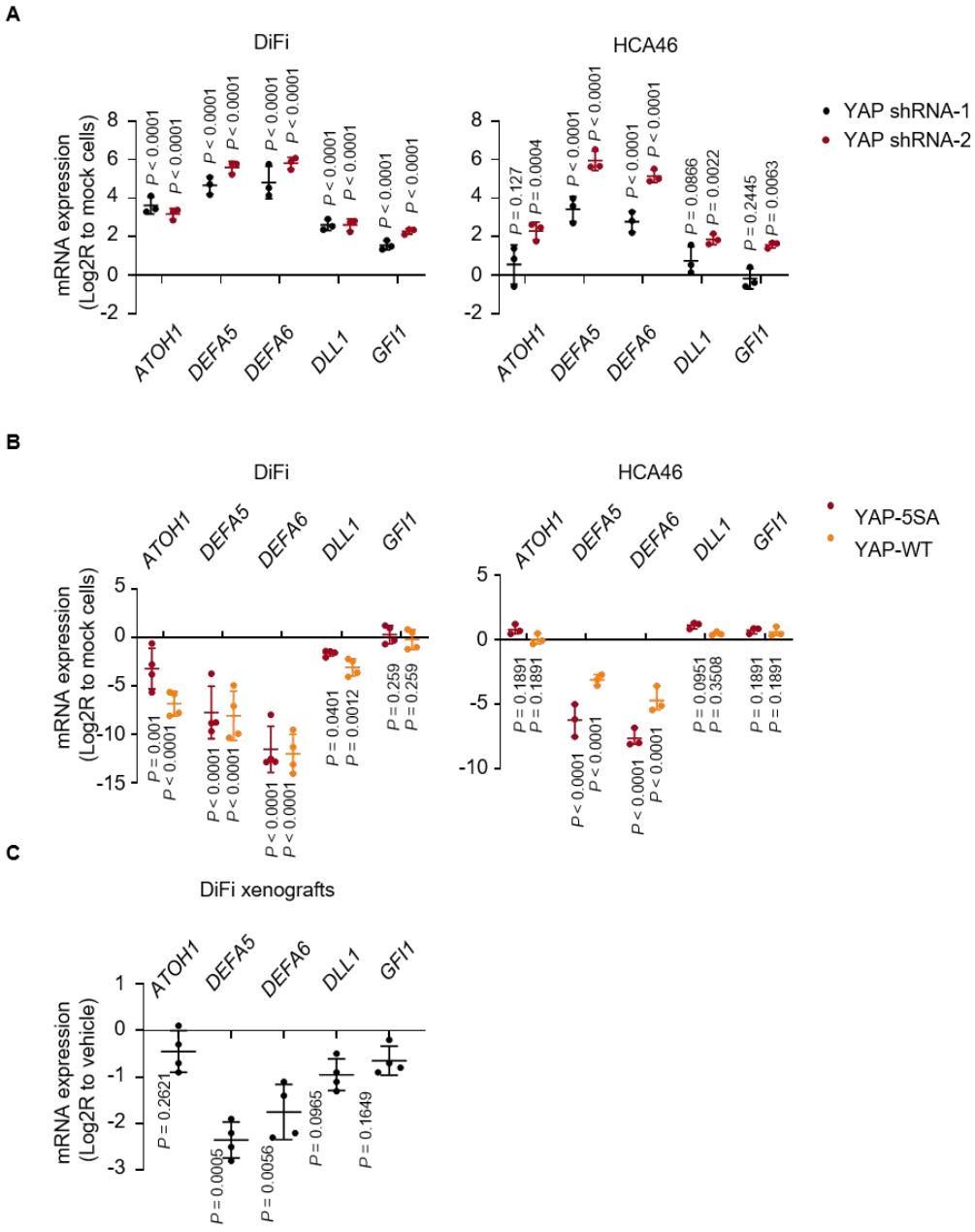

Figure S14. Expression of secretory/Paneth cell genes after YAP silencing or YAP overexpression in vitro and in vivo

(**A**) RT-qPCR analysis of the indicated secretory/Paneth-cell genes in DiFi and HCA46 cells after shRNA-based YAP silencing, compared with mock cells. Three independent experiments were performed in technical triplicates. (**B**) RT-qPCR analysis of the indicated secretory/Paneth-cell genes in DiFi and HCA46 cell lines transduced with YAP-5SA or YAP-WT. Four (DiFi) or 3 (HCA46) independent experiments were performed in technical triplicates. To quantitate gene expression downregulation, technical triplicates consisting of one or two undetermined cycle threshold (Ct) values together with one or two detectable Ct > 37 were equalized to a Ct value of 40. (**C**) RT-qPCR analysis of the indicated secretory/Paneth-cell genes in established DiFi xenografts

transduced with doxycycline-inducible YAP-5SA and treated with doxycycline (50 mg/kg daily). Four samples for each condition were analyzed in technical triplicates. In all panels, the plots show means ± SD. For all experiments, statistical analysis was performed by one-way ANOVA followed by Benjamini, Krieger and Yekutieli FDR correction.

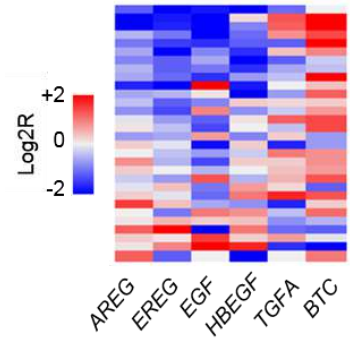

Figure S15. Modulation of EGFR family ligands in PDXs treated with cetuximab

Heatmap showing expression changes for the indicated EGFR ligands in PDXs of the reference collection, after treatment with cetuximab, as assessed by RT-qPCR. Average gene expression, Log2R relative to vehicle-treated tumors: *AREG* -0.28, *P* = 0.206; *EREG* -0.71, *P* = 0.004; *EGF* -0.67, *P* = 0.349; *HBEGF* -0.56, *P* = 0.220; TGFα (*TGFA*) -0.1, *P* = 0.766; *BTC* 0.6, *P* = 0.001 by two-tailed Wilcoxon test. Benjamini-Hochberg FDR < 0.1 for *EREG* and *BTC*.

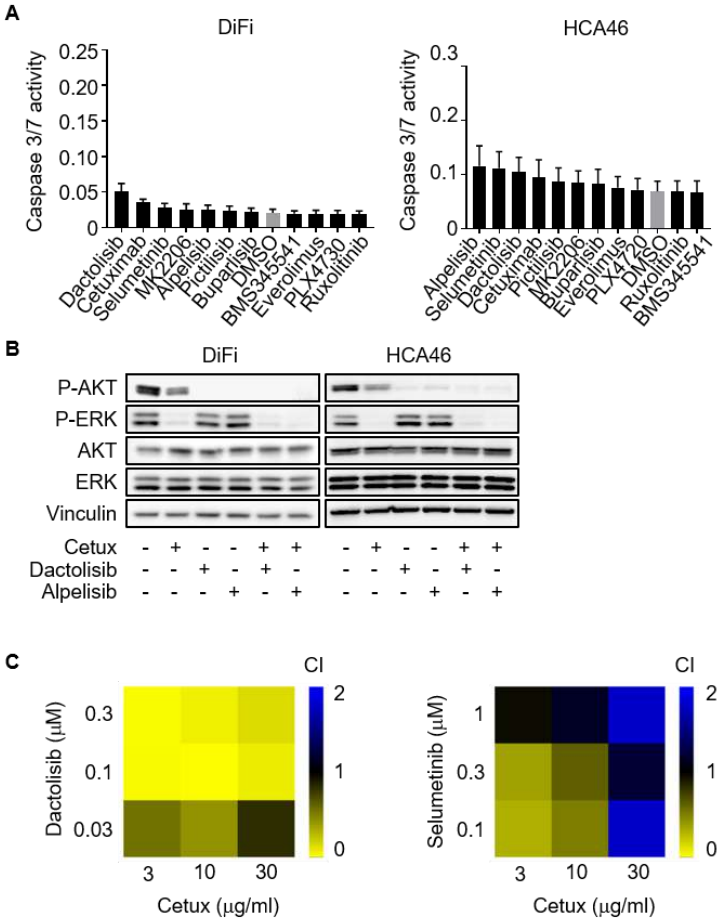

Figure S16. Effects of individual signal inhibition and dual blockade of EGFR and PI3K or EGFR and MEK in CRC cell cultures

(**A**) Luciferase-based evaluation of apoptosis (assessed by caspase 3/7 activity) in DiFi and HCA46 cell lines either left untreated (vehicle, DMSO, grey bars) or exposed for 24h to the indicated drugs, used as monotherapy at the following concentrations: cetuximab, 20 μg/ml; BMS345541 (IkB/IKK inhibitor), ruxolitinib (JAK1/JAK2 inhibitor), selumetinib (MEK1 inhibitor), PLX4720 (BRAF inhibitor), alpelisib (PI3Kα inhibitor), 1 μM; dactolisib (PI3K/mTOR inhibitor), 250 nM; everolimus (mTOR inhibitor), 50 nM; pictilisib (PI3Kα/δ inhibitor), 100 nM; MK2206 (AKT inhibitor), 0.5 μM; buparlisib (Pan-PI3K inhibitor), 0.5 μM. Results represent the means ± SD of 2 independent experiments performed in biological quintuplicates (*n* = 10). Values shown for cetuximab monotherapy and Y axis scale are the same as in main Figure 5 for comparative purposes. (**B**) Western blot analysis of AKT and ERK phosphorylation in DiFi and HCA46 cell lines treated for 2 h with dactolisib (250 nM), alpelisib (1 μM) and/or for 24 h with cetuximab (20 μg/ml). Total ERK and AKT were used for normalization; vinculin was used as a loading control. Western blots for total proteins were run with the same lysates as those used for anti-phosphoprotein detection but on different gels. The images shown are representative of 2 experiments on independent biological replicates. Cetux, cetuximab. P-AKT, phospho-AKT; P-ERK, phospho-ERK. (**C**) Analysis of

combination index (CI) to assess drug interaction effects in CRC0078 colospheres embedded in PuraMatrix and treated for 2 weeks with the indicated drugs and concentrations. A dose-response matrix design was applied, and CI values were calculated by the Compusyn software using the equatorial areas of colospheres as proxies of cell viability. CI > 1 designates antagonism, CI = 1 indicates an additive effect, and CI < 1 is defined as synergy. Cetuximab and dactolisib exhibited a synergistic effect at all concentrations tested (CI ranging from 0.007 to 0.822). The synergy between cetuximab and selumetinib occurred only at low compound concentrations and was less pronounced (CI ranging from 0,312 to 1,786).

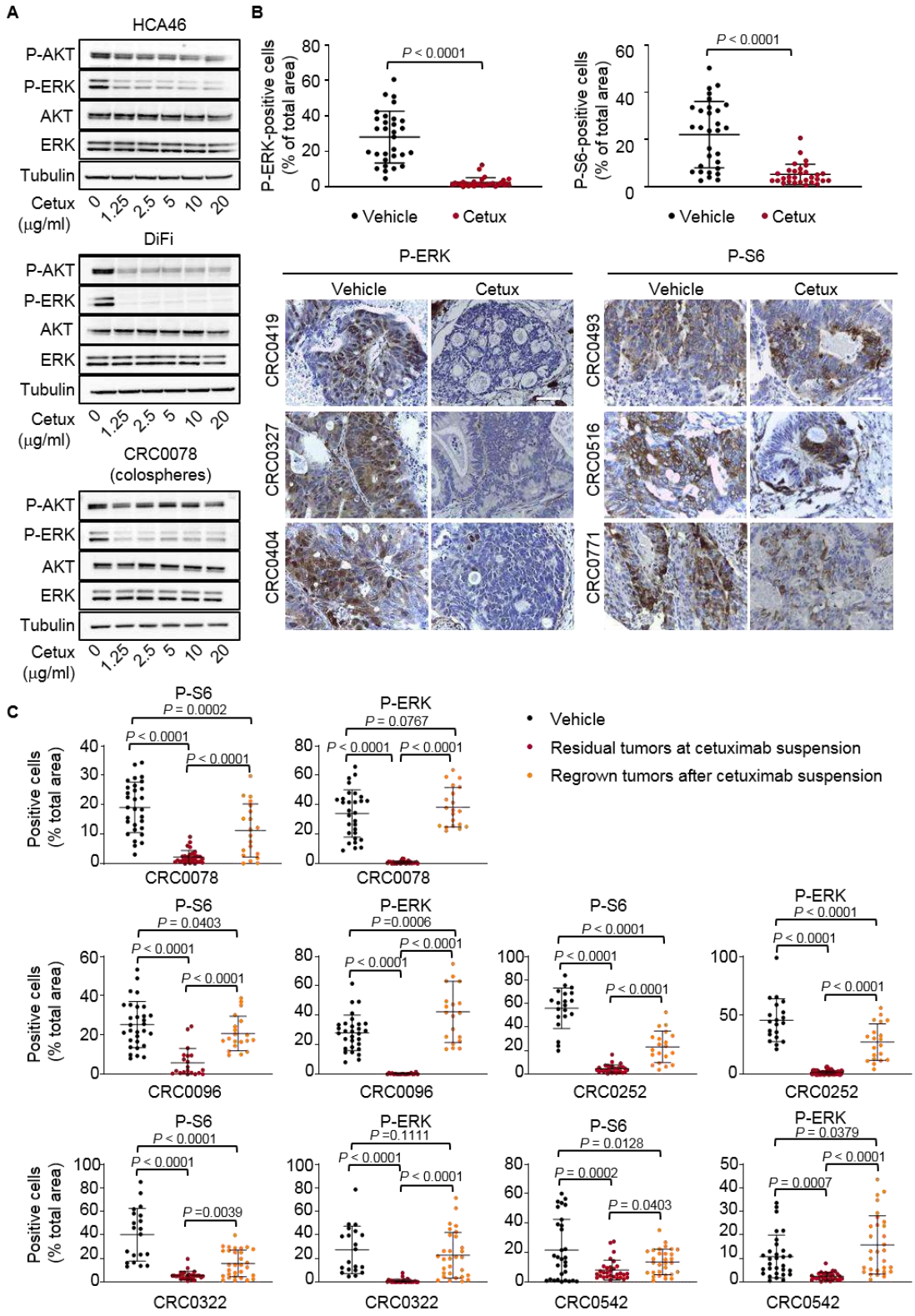

Figure S17. Effects of cetuximab on downstream signals in vitro and in vivo

(**A**) Western blot analysis of AKT and ERK phosphorylation in DiFi and HCA46 cell lines and in CRC0078 colospheres treated for 24h (cell lines) or 72h (CRC0078) with cetuximab at the indicated

concentrations. Total ERK and AKT were used for normalization; tubulin was used as a loading control. Western blots for total proteins were run with the same lysates as those used for anti-phosphoprotein detection but on different gels. The images shown are representative of 2 (DiFi, HCA46) or 3 (CRC0078) experiments on independent biological replicates. Cetux, cetuximab; P-ERK, phospho-ERK; P-AKT, phospho-AKT. (**B**) Morphometric quantitation (upper panels) and representative images (lower panels) of phospho-ERK and phospho-S6 immunoreactivity in PDXs from the reference collection after treatment with vehicle (until tumors reached an average volume of 1500 mm^3) or cetuximab (20 mg/kg twice a week for 6 weeks). Each dot represents the average of 10 optical fields (40X) in a section from randomly chosen tumors from vehicle-treated and cetuximab-treated mice bearing a PDX from the same original patient (n = 30). The plots show means ± SD. Statistical analysis by two-tailed paired Student's t-test. Scale bar, 50 μm. P-S6, phospho-S6. (**C**) Morphometric quantitation of phospho-S6 and phospho-ERK immunoreactivity in 5 representative PDX models after treatment with vehicle (until tumors reached an average volume of 1500 mm^3) or cetuximab (20 mg/kg twice a week for 6 weeks). Results are also shown for matched cases after antibody withdrawal, when regrown tumors reached volumes of around 750 mm^3. At endpoints, 3 tumors from 3 different mice were explanted and subjected to immunohistochemical analysis. Each dot represents the value measured in one optical field (40x), with 2 to 10 optical fields per tumor depending on the extent of section area (n = 20 to 30). The plots show means ± SD. Statistical analysis by one-way ANOVA followed by Benjamini, Krieger and Yekutieli FDR correction.

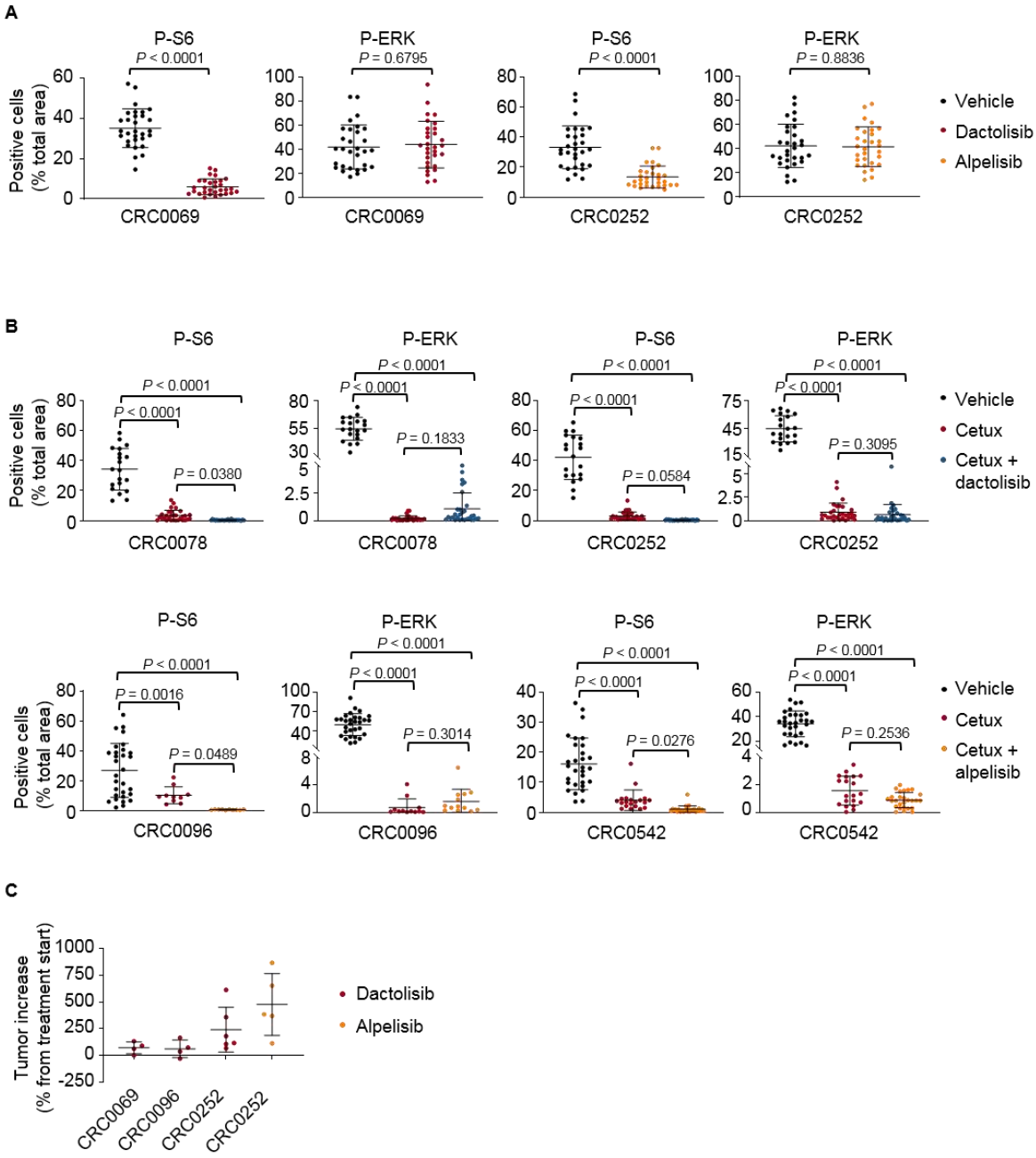

Figure S18. Effects of PI3K inhibitors on downstream signals and tumor growth in vivo

(**A**) Morphometric quantitation of phospho-S6 and phospho-ERK immunoreactivity in PDXs treated with vehicle (until tumors reached an average volume of 1500 mm^3), dactolisib alone (35 mg/Kg, daily oral gavage) or alpelisib alone (25 mg/Kg, daily oral gavage) for 4 weeks (CRC0069) or 3 weeks (CRC0252). In the case of CRC0252, the experiment was terminated at 3 weeks because some mice had to be euthanized upon reaching of the humane endpoint. (**B**) Morphometric quantitation of phospho-S6 and phospho-ERK immunoreactivity in PDXs treated with vehicle (until tumors reached an average volume of 1500 mm^3), cetuximab alone (4 weeks), cetuximab and dactolisib (4 weeks) or cetuximab and alpelisib (4 weeks). Cetuximab, 20 mg/Kg (intraperitoneal

injection twice a week); dactolisib, 35 mg/Kg (daily oral gavage); alpelisib, 25 mg/Kg (daily oral gavage). In both (**A**) and (**B**), at the end of treatment 3 tumors from 3 different mice (2 tumors from 2 different mice in CRC0096 treated with alpelisib and cetuximab) were explanted and subjected to immunohistochemical analysis. Each dot represents the value measured in one optical field (40x), with 3 to 10 optical fields per tumor depending on the extent of section area (n = 10 to 30). The plots show means ± SD. Statistical analysis by two-tailed unpaired Welch's t-test (**A**) or one-way ANOVA followed by Benjamini, Krieger and Yekutieli FDR correction (**B**). (**C**) Tumor volume changes in the indicated cases treated with dactolisib alone or alpelisib alone for 4 weeks (CRC0069, CRC0096) or 3 weeks (CRC0252). Dots represent volume changes of individual mice, and plots show the means ± SD. n = 4 to 6 animals per each treatment arm.

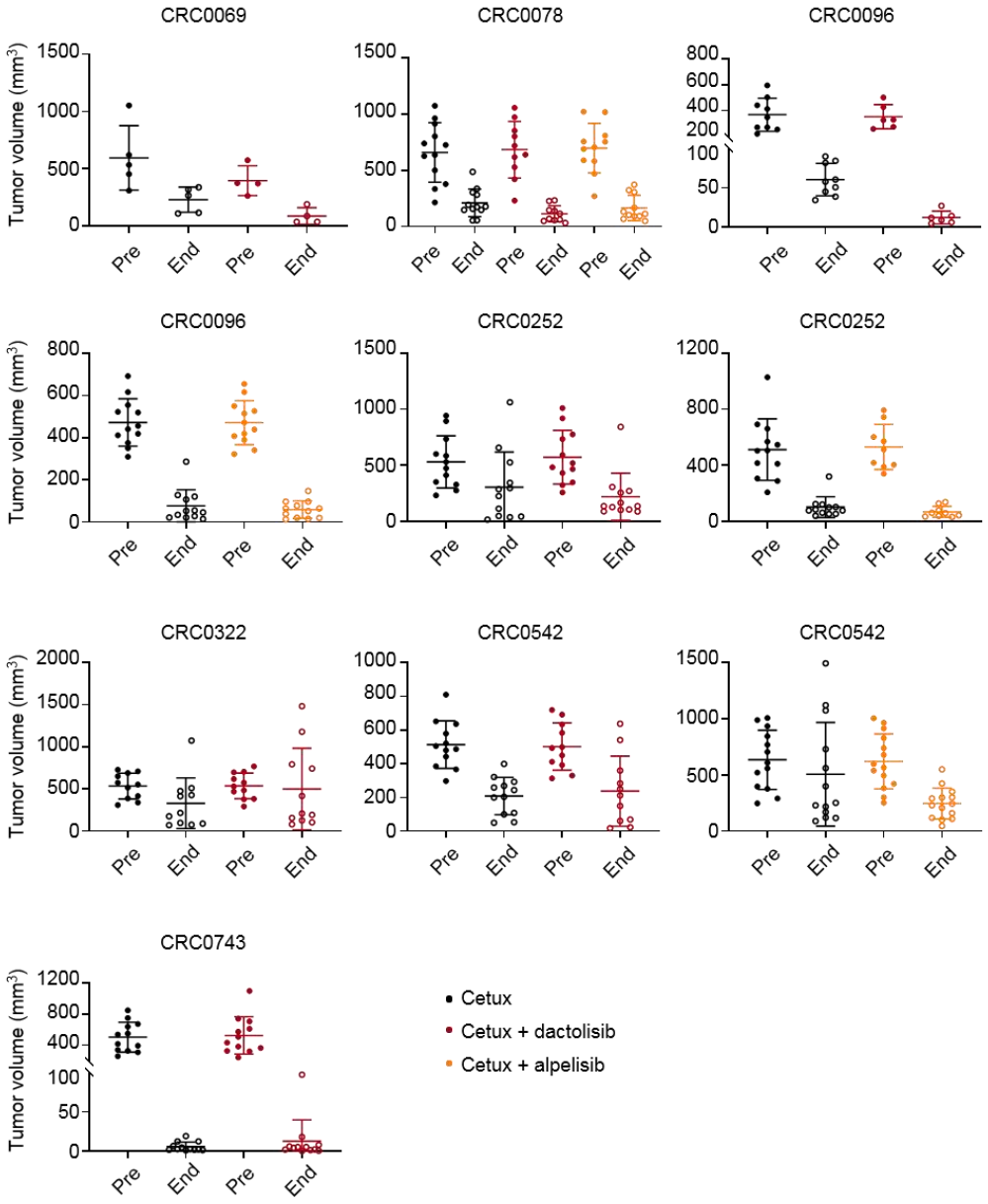

Figure S19. Effects of PI3K inhibition and combined EGFR and PI3K inhibition on mCRC PDX macroscopic residual disease (pre-treatment and end-of-treatment tumor volumes)

Tumor volumes in PDXs treated with the indicated modalities for 4 weeks. Cetuximab, 20 mg/Kg (intraperitoneal injection twice a week); dactolisib, 35 mg/Kg (daily oral gavage); alpelisib, 25 mg/Kg (daily oral gavage). Dots represent tumor volumes in individual mice, and plots show the means ± SD for each treatment arm. *n* = 4 to 14 animals per each treatment arm. Cetux, cetuximab; Pre, pre-treatment (day 0); End, end-of-treatment (4 weeks).

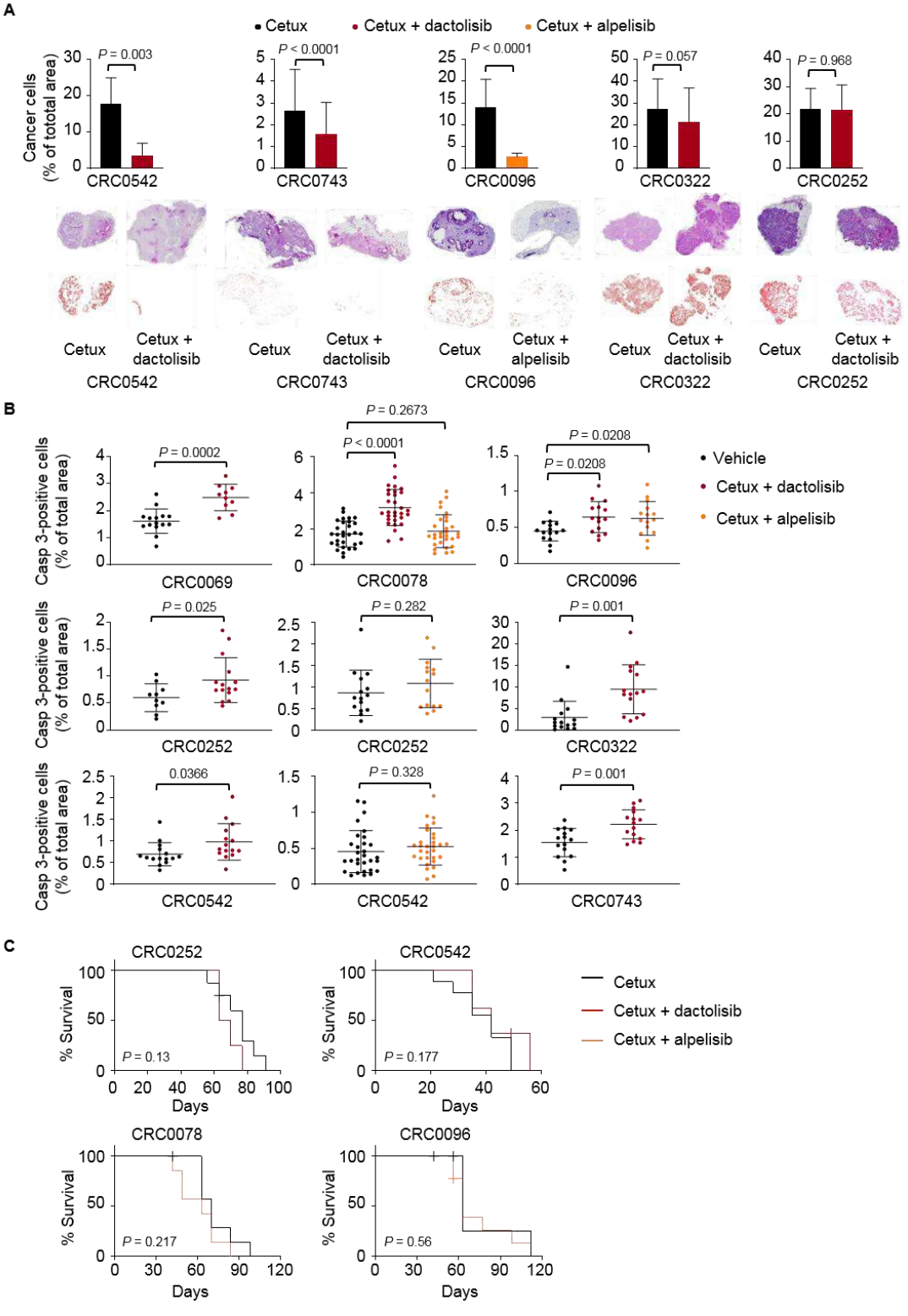
A
Cetux
Cetux + dactolisib
Cetux + alpelisib
Cancer cells (% of totoal area)
P = 0.003
P < 0.0001
P < 0.0001
P = 0.057
P = 0.968
CRC0542
CRC0743
CRC0096
CRC0322
CRC0252
Cetux
Cetux + dactolisib
Cetux + alpelisib
B
Casp 3-positive cells (% of total area)
P = 0.0002
P = 0.2673
P < 0.0001
P = 0.0208
P = 0.0208
P = 0.025
P = 0.282
P = 0.001
0.0366
P = 0.328
P = 0.001
CRC0069
CRC0078
CRC0096
CRC0252
CRC0252
CRC0322
CRC0542
CRC0542
CRC0743
Vehicle
Cetux + dactolisib
Cetux + alpelisib
C
CRC0252
CRC0542
CRC0078
CRC0096
% Survival
Days
P = 0.13
P = 0.177
P = 0.217
P = 0.56
Cetux
Cetux + dactolisib
Cetux + alpelisib

Figure S20. Effects of combined EGFR and PI3K inhibition on mCRC PDX microscopic residual disease, apoptosis, and survival

(**A**) Microscopic assessment of residual cancer cell burden in PDXs treated with the indicated modalities for 4 weeks. Cetuximab, 20 mg/Kg (intraperitoneal injection twice a week); dactolisib, 35 mg/Kg (daily oral gavage); alpelisib, 25 mg/Kg (daily oral gavage). Upper panels indicate morphometric quantitations (n = 4 to 89 depending on the extent of section area); lower panels include hematoxylin-and-eosin staining and visualization of cancer cells (in brown) by digital segmentation. Statistical analysis by two-tailed unpaired Welch's t-test. Cetux, cetuximab. (**B**) Morphometric quantitation of apoptosis (caspase 3 staining) in PDXs treated for 24 hours with the indicated modalities. After treatment, 3 tumors from 3 different mice were explanted and subjected to immunohistochemical analysis. Each dot represents the value measured in one optical field (20x), with 3 to 10 optical fields per tumor depending on the extent of section area (n = 10 to 30). The plots show means ± SD. For CRC0069, CRC0252, CRC0322, CRC0542, and CRC0743, statistical analysis was performed by two-tailed unpaired Welch's t-test. For CRC0096 and CRC0078, statistical analysis was performed by one-way ANOVA followed by Benjamini, Krieger and Yekutieli FDR correction. Casp, caspase. (**C**) Kaplan-Meier survival curves in PDXs after discontinuation of the indicated treatments. n = 6 to 9 animals per each treatment arm. Statistical analysis by Log-rank (Mantel-Cox) test.

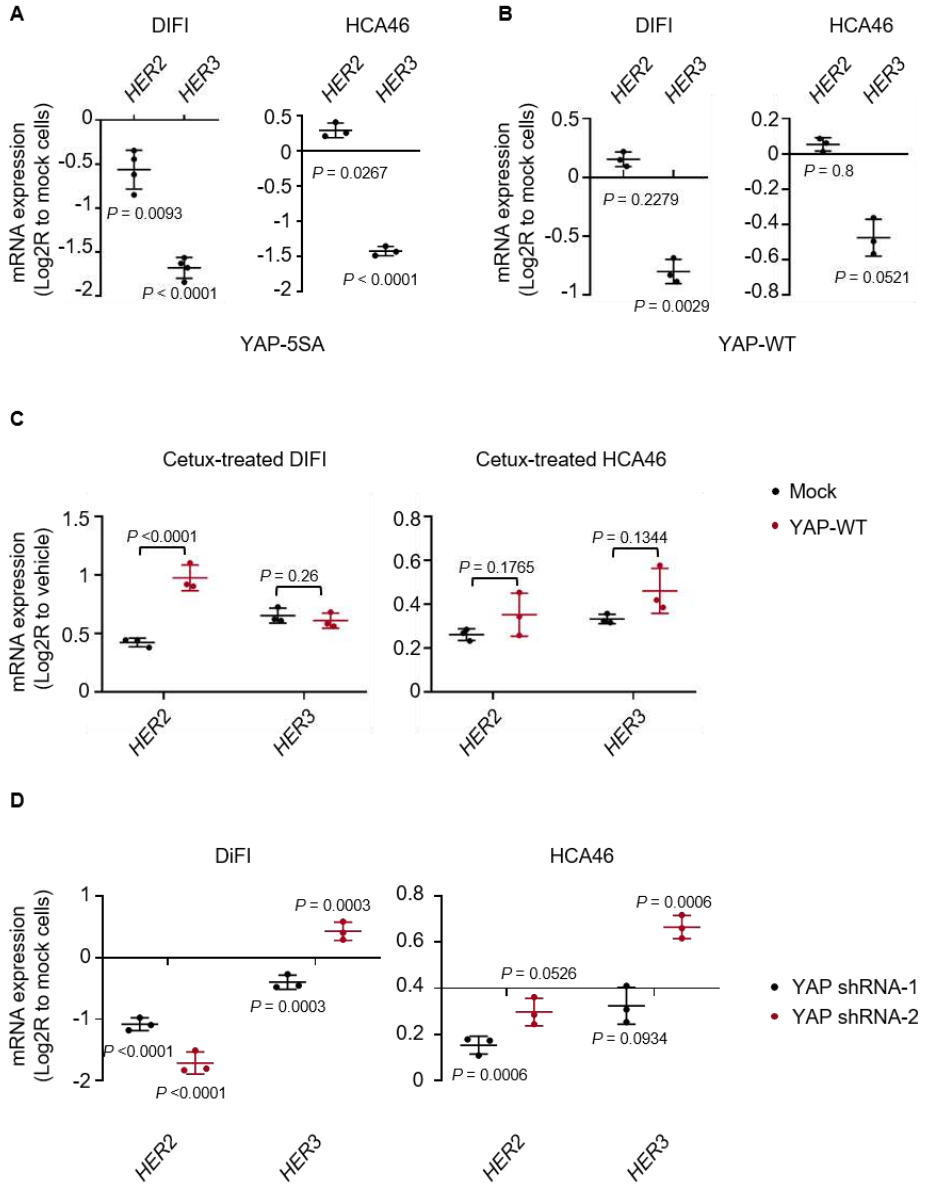

Figure S21. YAP-dependent transcriptional modulation of *HER2* and *HER3* in CRC cell lines

(**A** and **B**) RT-qPCR analysis of *HER2* and *HER3* transcript expression in DiFi and HCA46 cell lines transduced with constitutive active YAP (YAP-5SA) (**A**) or wild-type YAP (YAP-WT) (**B**). (**C**) RT-qPCR analysis of *HER2* and *HER3* transcript expression in DiFi and HCA46 cell lines transduced with a pLVX-control vector (mock) or wild-type YAP (YAP-WT), and treated with cetuximab (20 µg/ml) for 72h. (**D**) RT-qPCR analysis of *HER2* and *HER3* transcript expression in DiFi and HCA46 cells after shRNA-based YAP silencing, compared with mock cells. In all panels, the plots show means ± SD. In panel (**A**), 4 (DiFi) or 3 (HCA46) independent experiments were performed in technical triplicates. In all other panels, 3 independent experiments were performed in technical triplicates. Statistical analysis was performed by one-way ANOVA followed by Benjamini, Krieger and Yekutieli FDR correction.

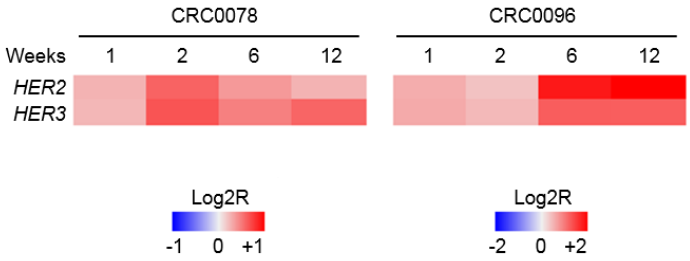

Figure S22. Modulation of *HER2* and *HER3* expression in PDXs during prolonged treatment with cetuximab

Heatmap showing expression changes for the indicated secretory/Paneth cell markers in 2 representative PDXs treated with cetuximab (20 mg/kg twice a week intraperitoneally) and monitored longitudinally for 12 weeks. At the indicated times, 1 tumor from 1 mouse was explanted and subjected to RT-qPCR analysis.

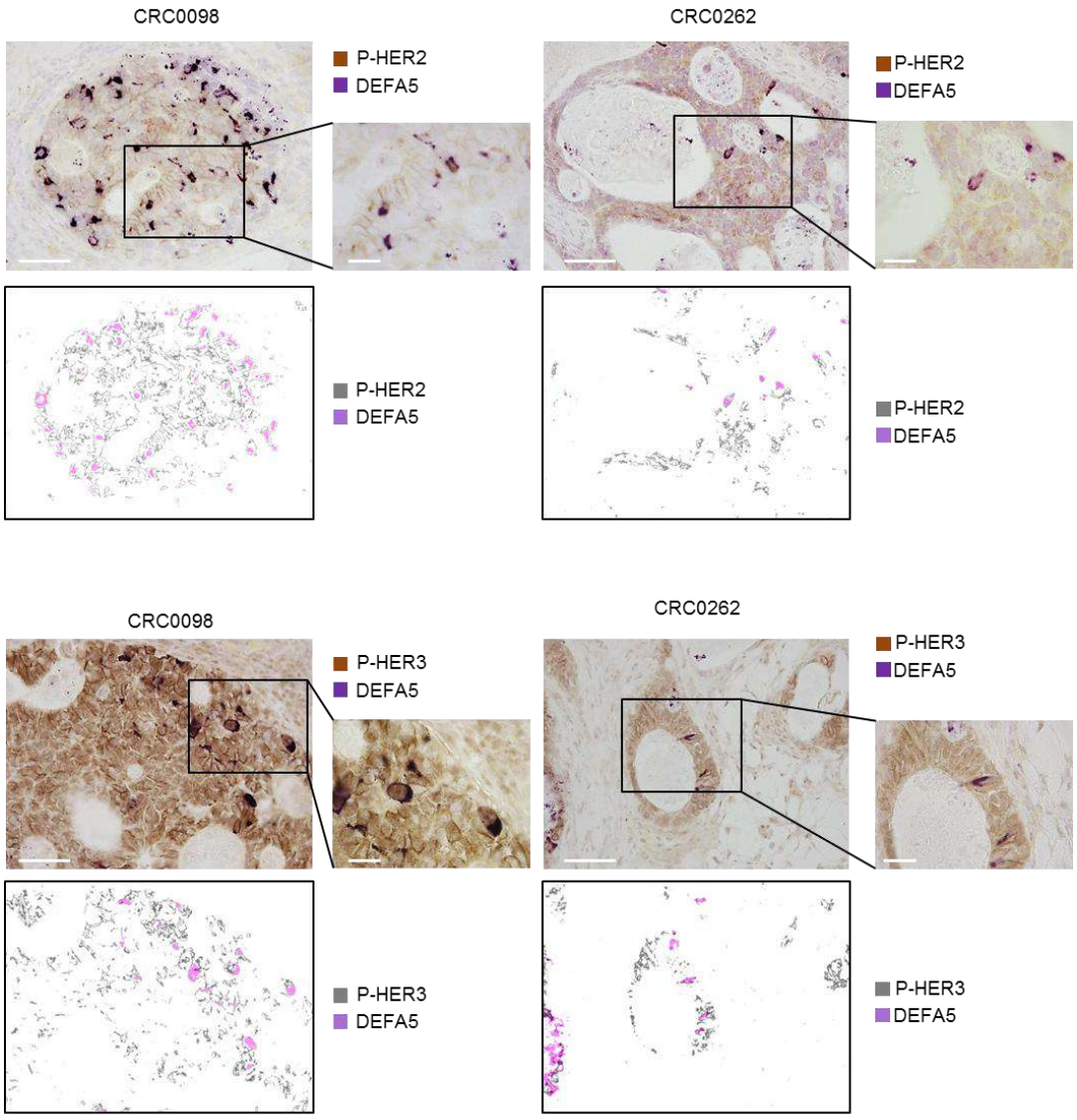

Figure S23. DEFA5 and HER2/HER3 double staining in representative mCRC PDXs treated with cetuximab

HER2 or HER3 and β-catenin double staining in 2 PDX models treated with cetuximab (20 mg/kg twice a week intraperitoneally) for 6 weeks. For each model, the upper panels are representative images of bright-field optical sections. The lower panels show the corresponding color deconvolution segmentation. Scale bar, 50 μM (insets, 20 μM). P-HER2, phoshpo-HER2; P-HER3, phospho-HER3.

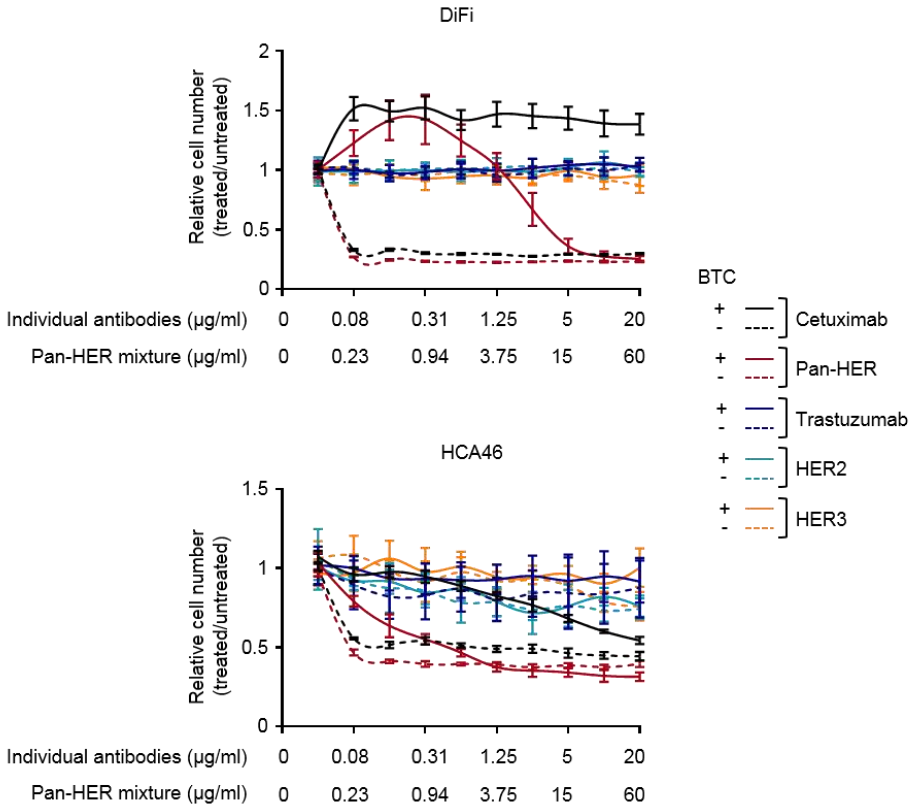

Figure S24. CRC cell line sensitivity to individual targeting of HER family members

Quantitation of cell number (assessed by ATP content) in DiFi and HCA46 cell lines treated for 72h with the indicated antibodies at the indicated concentrations in the absence or presence of 10 ng/ml BTC. Results represent the means ± SD of 2 independent experiments performed in biological triplicates (*n* = 6). HER2, anti-HER2 isolated component of Pan-HER; HER3, anti-HER3 isolated component of Pan-HER.

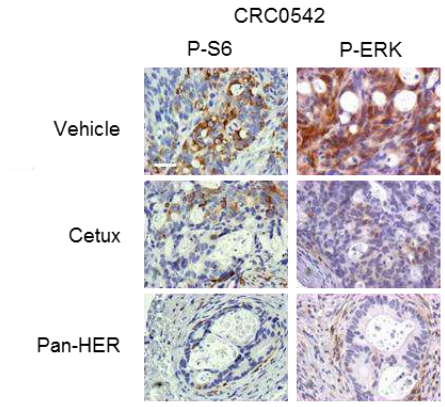

Figure S25. Effects of cetuximab and Pan-HER on EGFR downstream targets in vivo

Representative images (right panels) of phospho-S6 and phospho-ERK immunoreactivity (see main Figure 7 for quantitations) in PDXs after treatment with vehicle (until tumors reached an average volume of 1500 mm^3), cetuximab (20 mg/Kg, intraperitoneal injection twice a week for 5 weeks), or Pan-HER (60 mg/Kg, intraperitoneal injection twice a week for 5 weeks). At the end of treatment, 3 tumors from 3 different mice were explanted and subjected to immunohistochemical analysis. Cetux, cetuximab; P-S6, phospho-S6; P-ERK, phospho-ERK. Scale bar, 50 μm.